Supplementary material

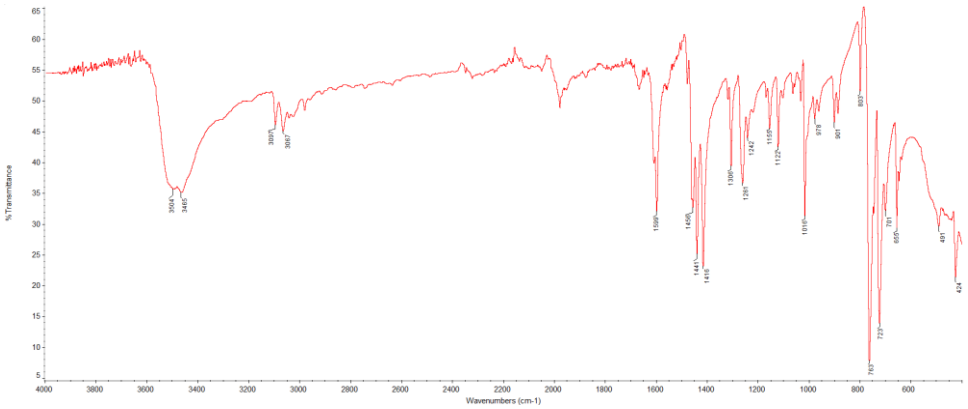

Figure S1 FTIR spectrum of precursor complex $[Ru(bipy)_2Cl_2]$

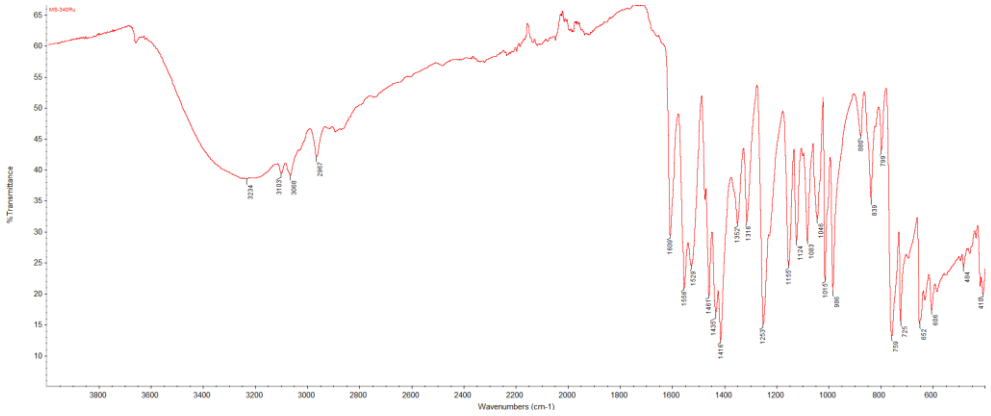

Figure S2 FTIR spectrum of complex [Ru(bipy)$_2$(4-F-Sal)]·3H$_2$O·EtOH (**1**·3H$_2$O·EtOH)

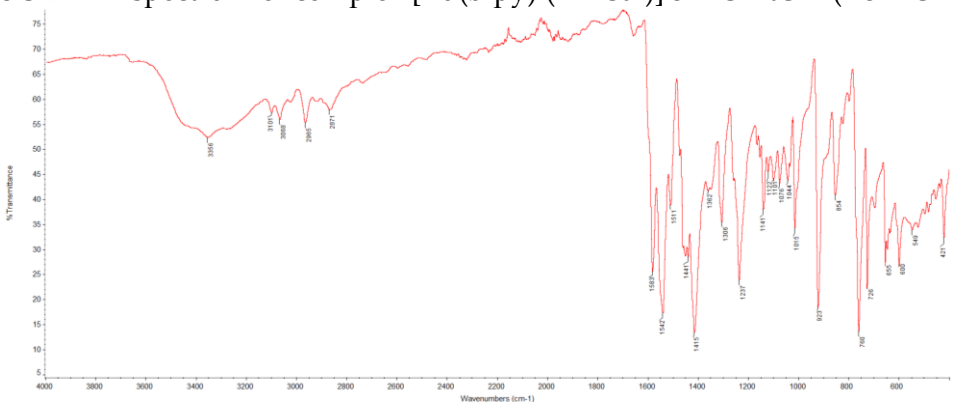

Figure S3 FTIR spectrum of complex [Ru(bipy)$_2$(4-Cl-Sal)]·2.6H$_2$O·2EtOH (**2**·2.6H$_2$O·2EtOH)

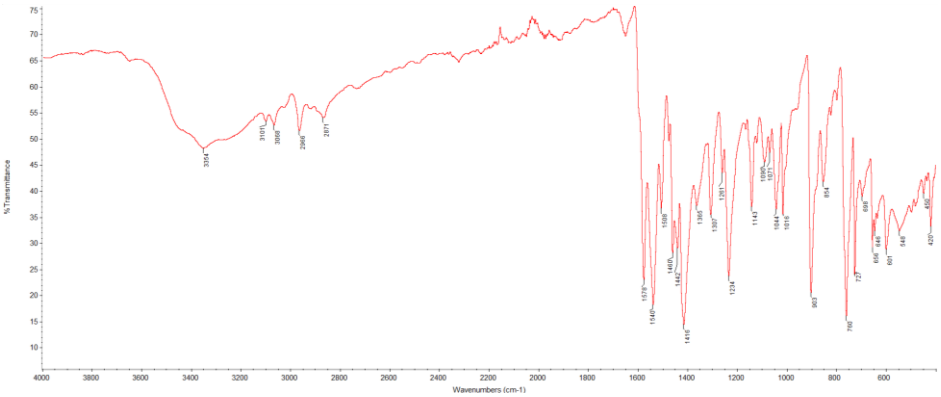

Figure S4 FTIR spectrum of complex [Ru(bipy)$_2$(4-Br-Sal)]·6H$_2$O (**3**·6H$_2$O)

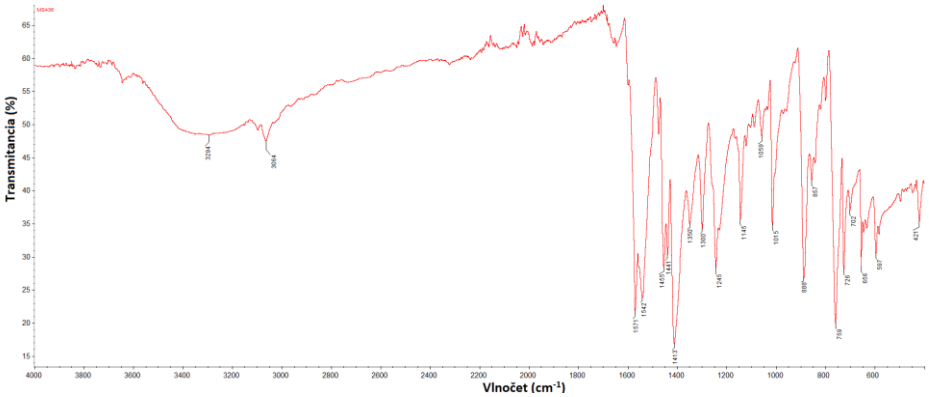

Figure S5 FTIR spectrum of complex [Ru(bipy)$_2$(4-I-Sal)]·3H$_2$O (**4**·3H$_2$O)

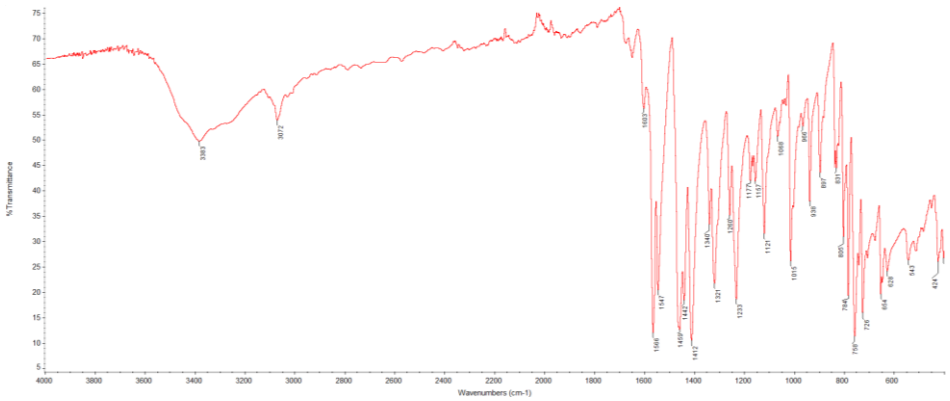

Figure S6 FTIR spectrum of complex [Ru(bipy)$_2$(5-F-Sal)]·1.55H$_2$O (**5**·1.55H$_2$O)

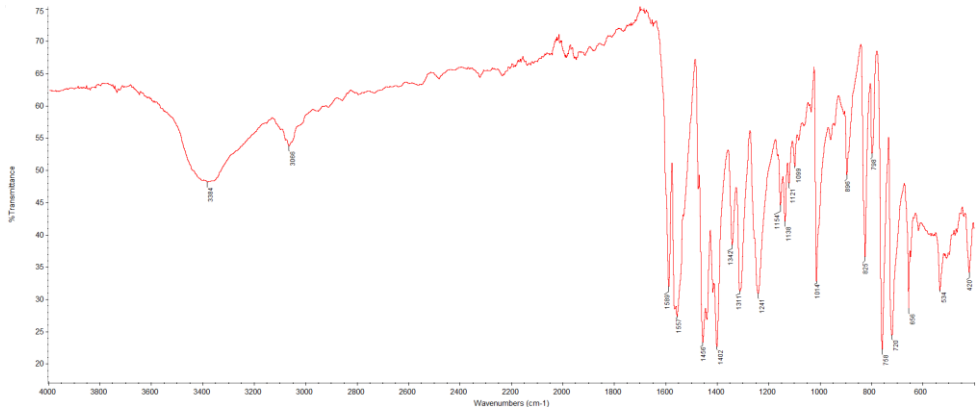

Figure S7 FTIR spectrum of complex [Ru(bipy)$_2$(5-Cl-Sal)] (**6**)

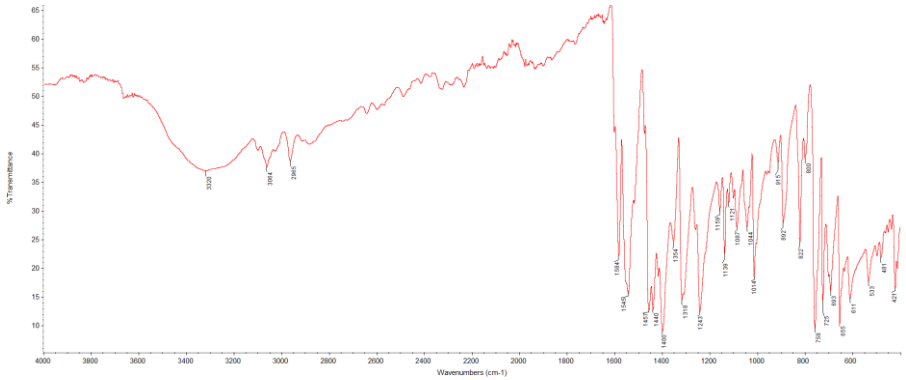

Figure S8 FTIR spectrum of complex [Ru(bipy)$_2$(5-Br-Sal)] (**7**)

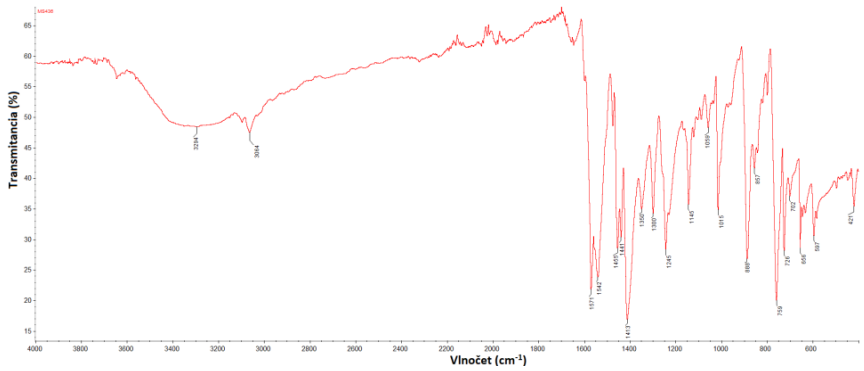

Figure S9 FTIR spectrum of complex [Ru(bipy)$_2$(5-I -Sal)]·4H$_2$O (**8**·4H$_2$O)

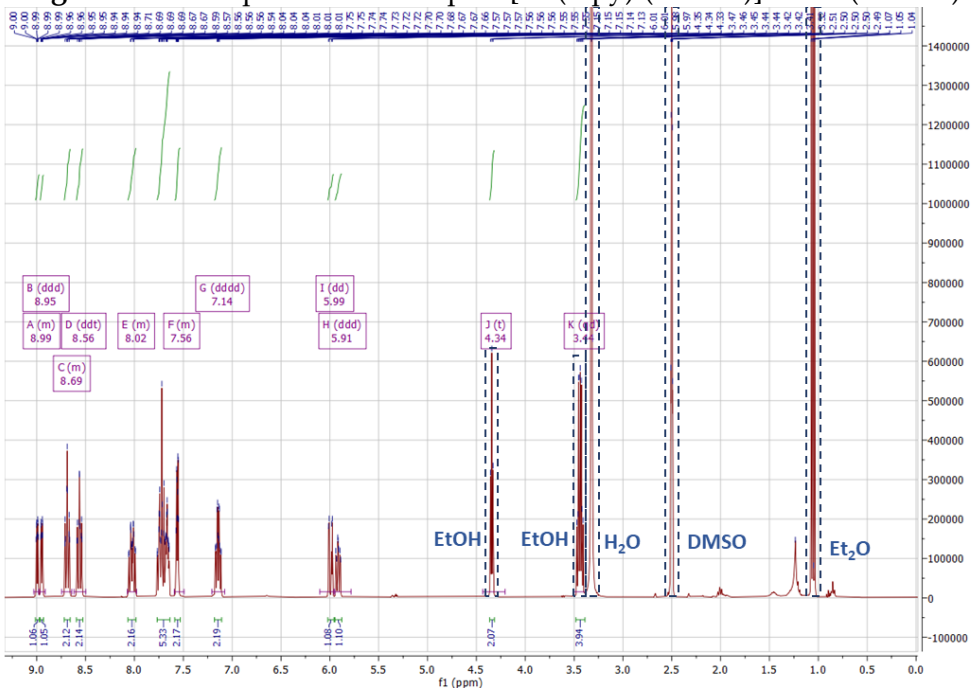

Figure S10 ^{1}H NMR spectrum of complex [Ru(bipy)$_2$(4-F-Sal)] (**1**) with marked signals for solvents and impurities (blue dashed line).

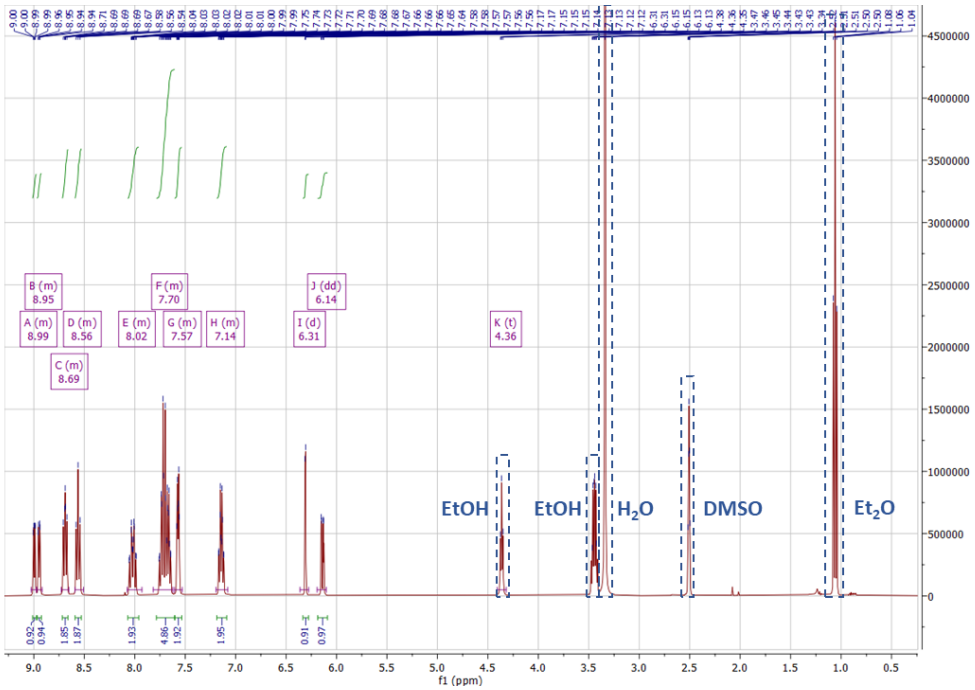

Figure S11 ^{1}H NMR spectrum of complex [Ru(bipy)$_2$(4-Cl-Sal)] (**2**) with marked signals for solvents and impurities (blue dashed line).

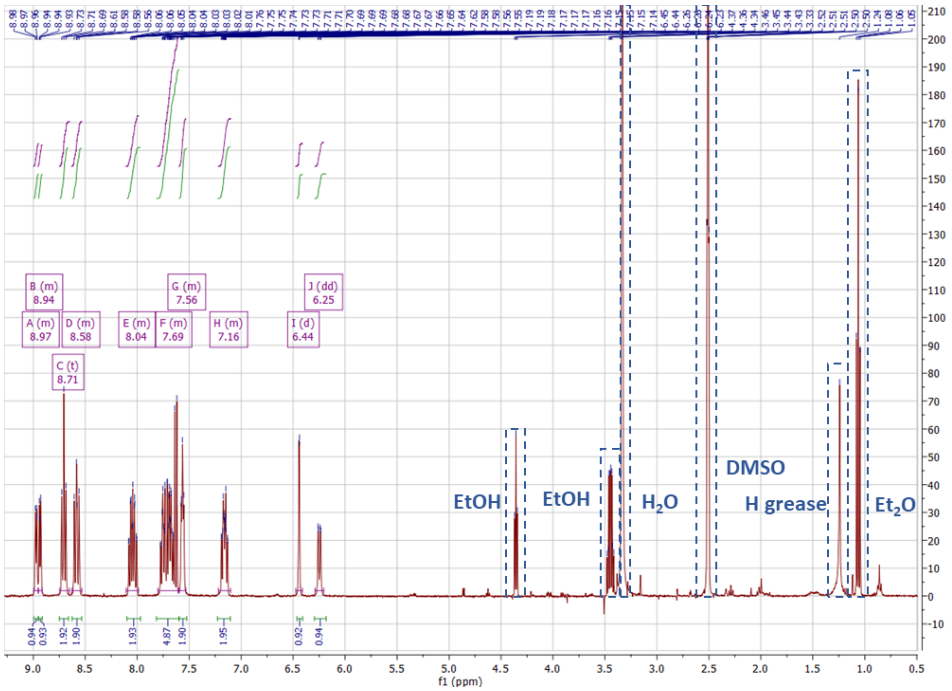

Figure S12 ^{1}H NMR spectrum of complex [Ru(bipy)$_2$(4-Br-Sal)] (**3**) with marked signals for solvents and impurities (blue dashed line).

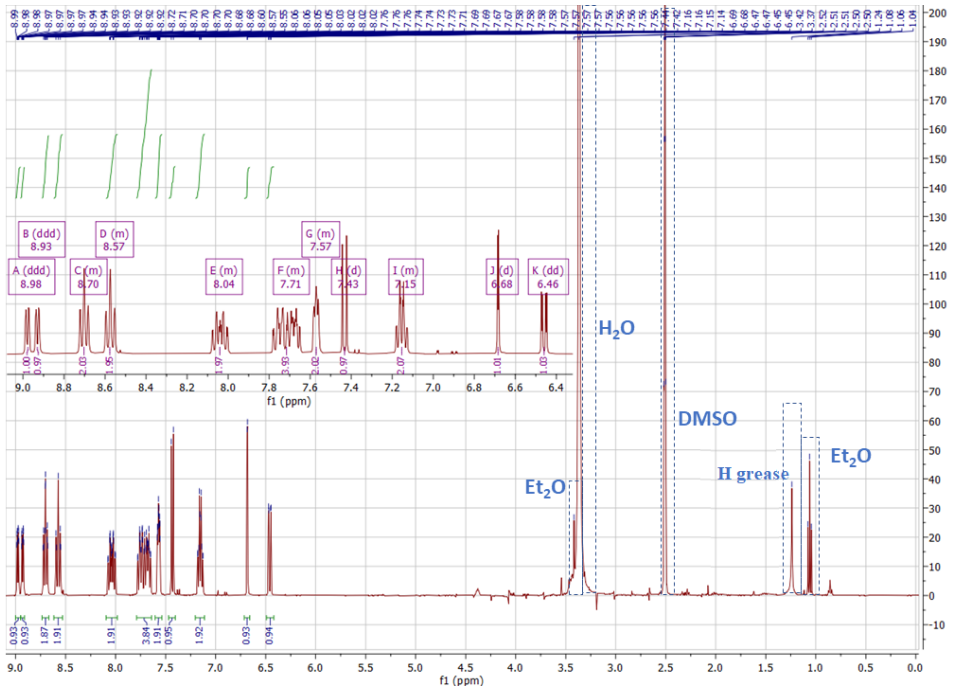

Figure S13 ^{1}H NMR spectrum of complex [Ru(bipy)$_2$(4-I-Sal)] (**4**) with marked signals for solvents and impurities (blue dashed line).

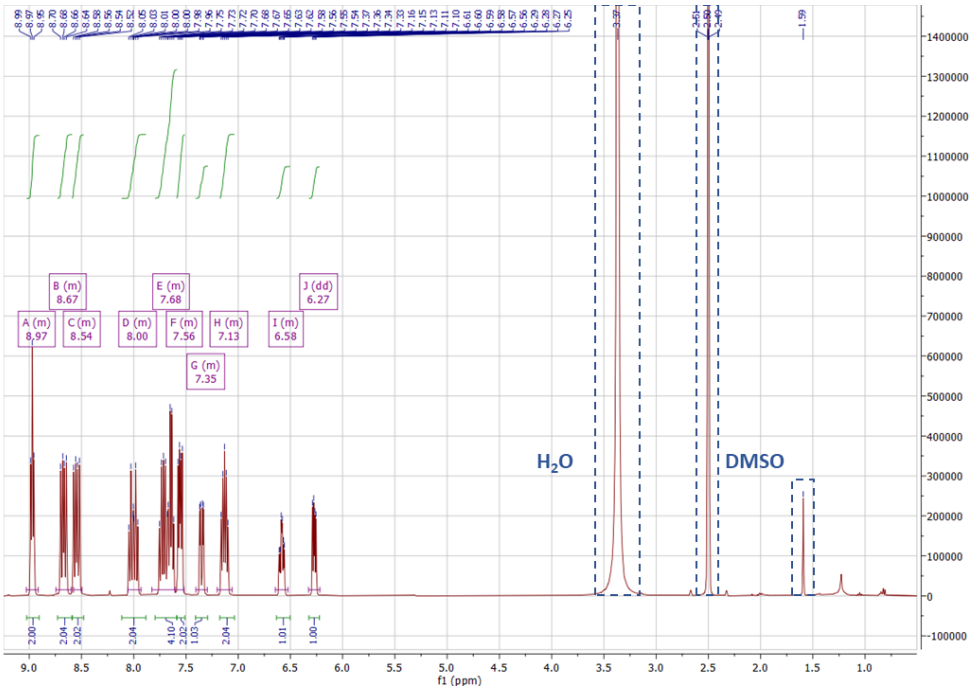

Figure S14 ^{1}H NMR spectrum of complex [Ru(bipy)$_2$(5-F-Sal)] (**5**) with marked signals for solvents and impurities (blue dashed line).

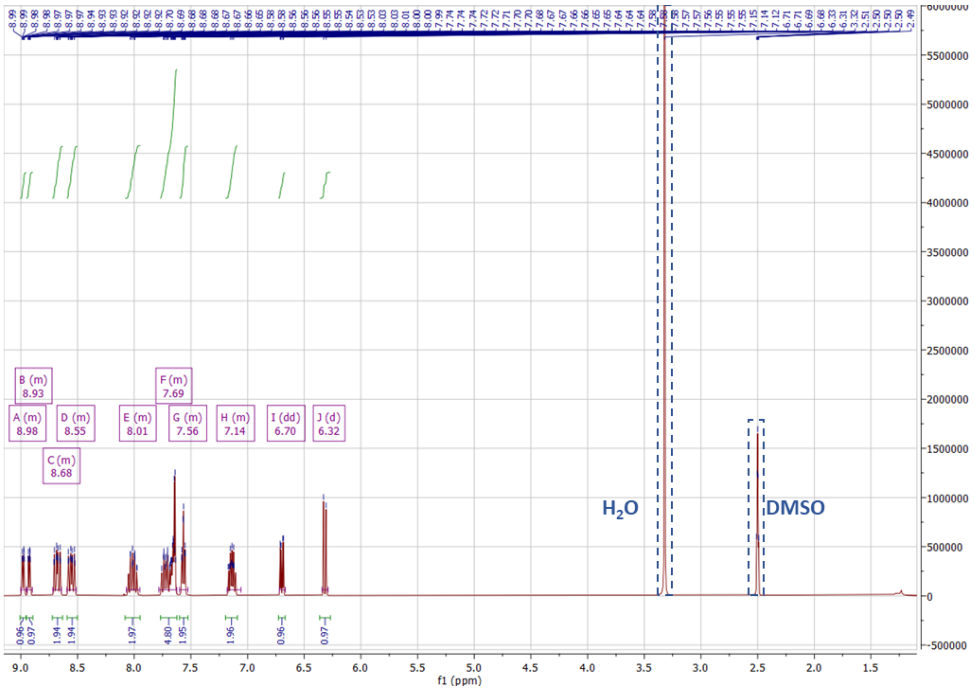

Figure S15 ^{1}H NMR spectrum of complex [Ru(bipy)$_2$(5-Cl-Sal)] (**6**) with marked signals for solvents and impurities (blue dashed line).

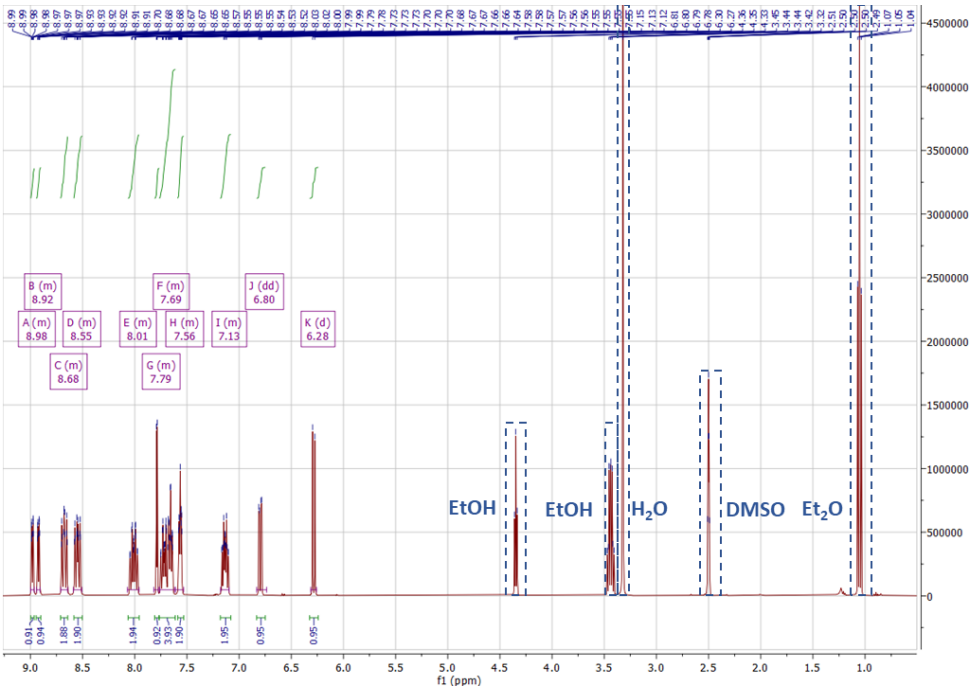

Figure S16 ^{1}H NMR spectrum of complex [Ru(bipy)$_2$(5-Br-Sal)] (**7**) with marked signals for solvents and impurities (blue dashed line).

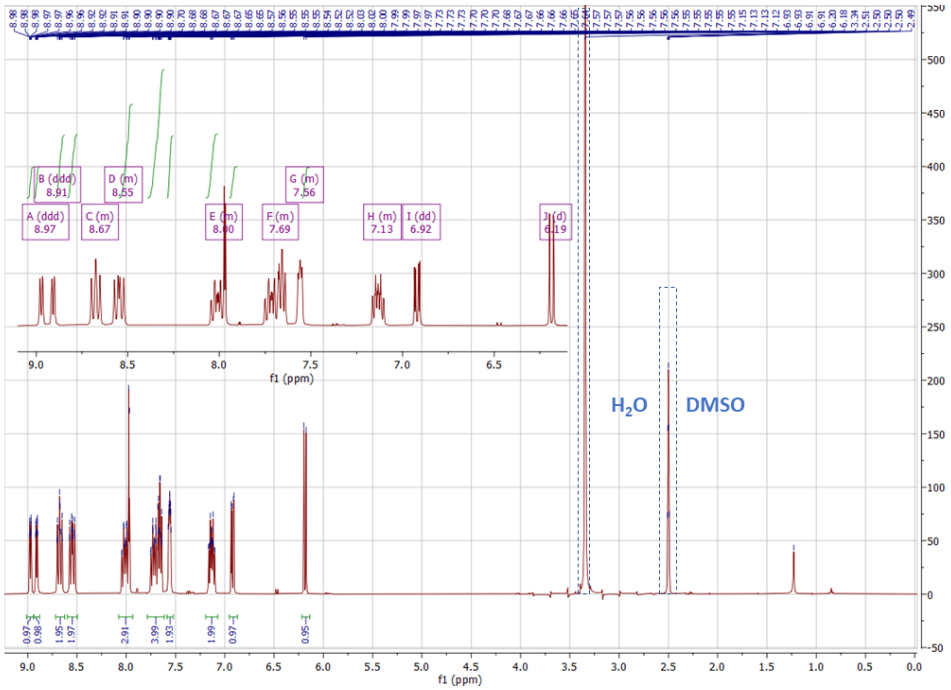

Figure S17 ^{1}H NMR spectrum of complex [Ru(bipy)$_2$(5-I-Sal)] (**8**) with marked signals for solvents and impurities (blue dashed line).

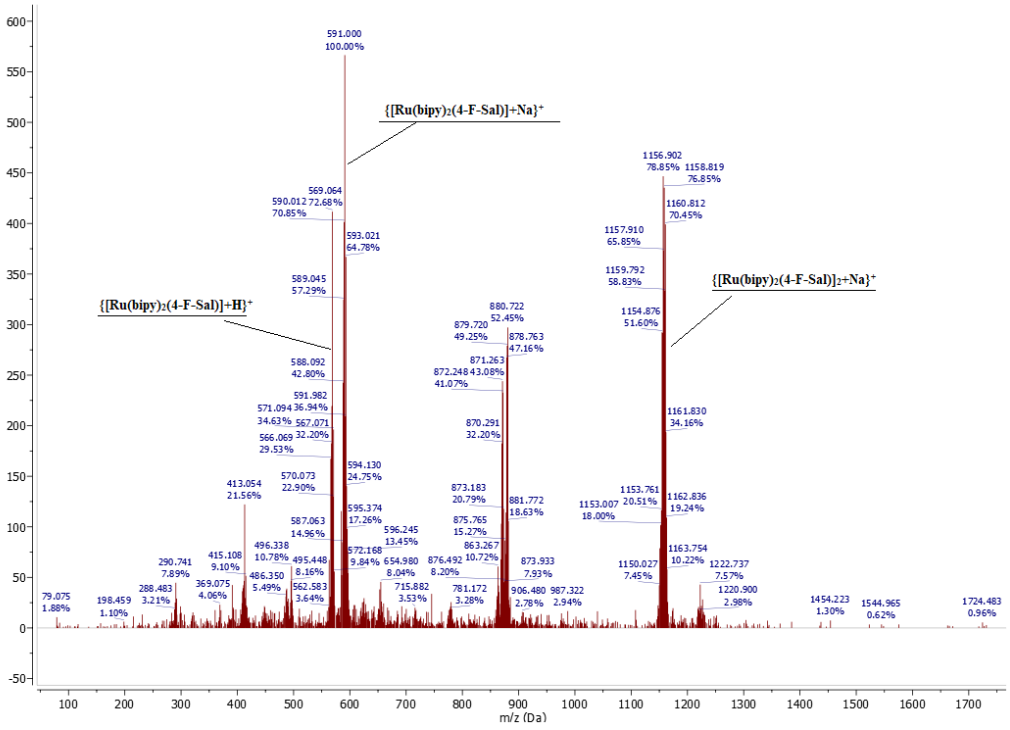

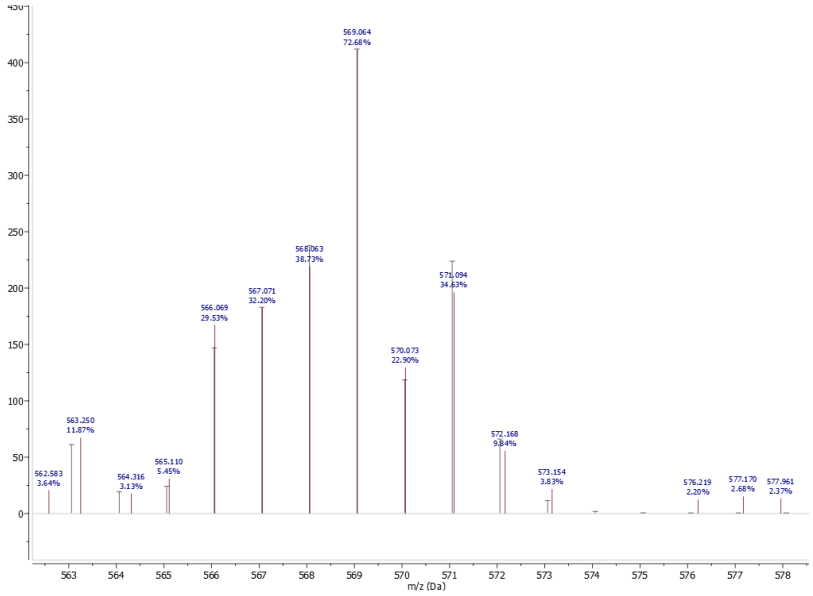

Figure S18 ESI-MS spectrum of complex [Ru(bipy)$_2$(4-F-Sal)] (**1**) together with the assignment of the most significant peaks. Below is a comparison of the simulated and measured isotope pattern for the molecular peak.

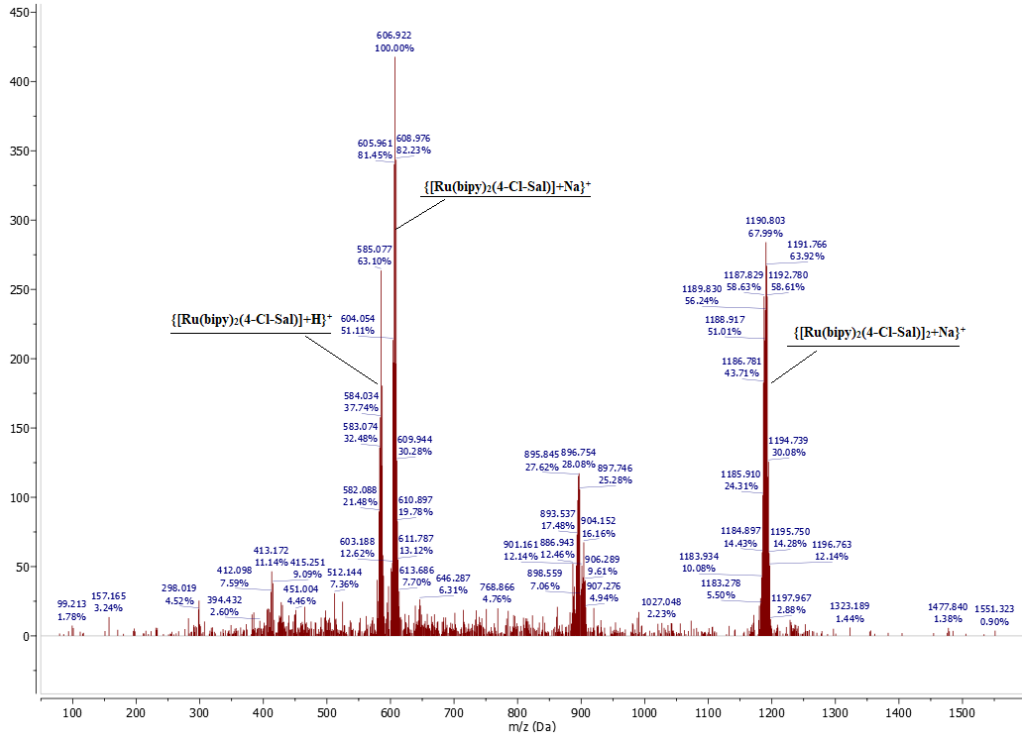

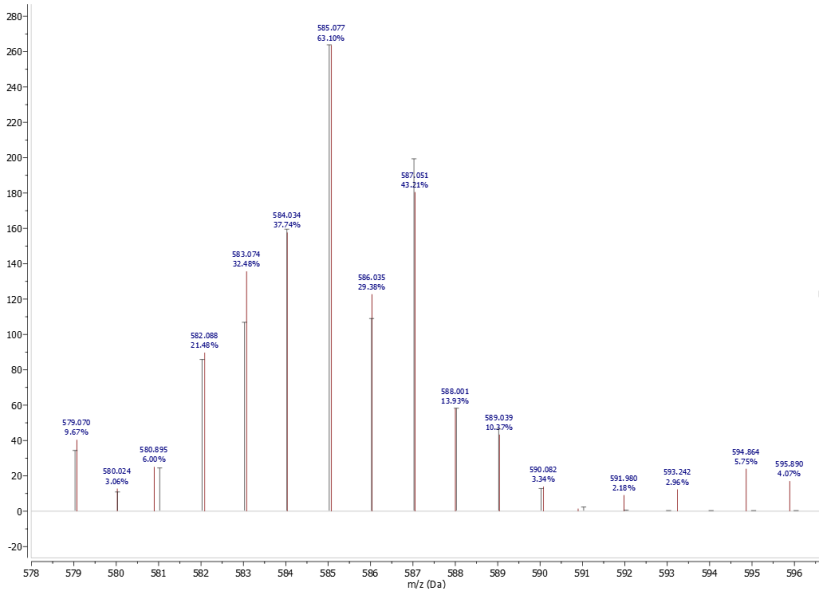

Figure S19 ESI-MS spectrum of complex [Ru(bipy)$_2$(4-Cl-Sal)] (**2**) together with the assignment of the most significant peaks. Below is a comparison of the simulated and measured isotope pattern for the molecular peak.

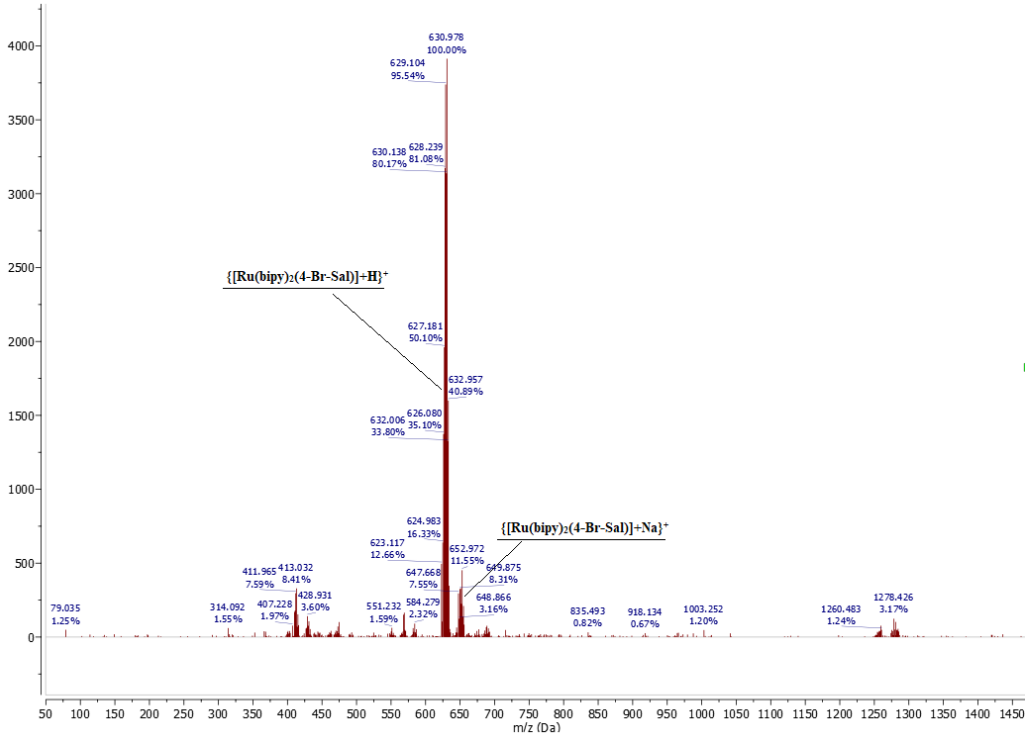

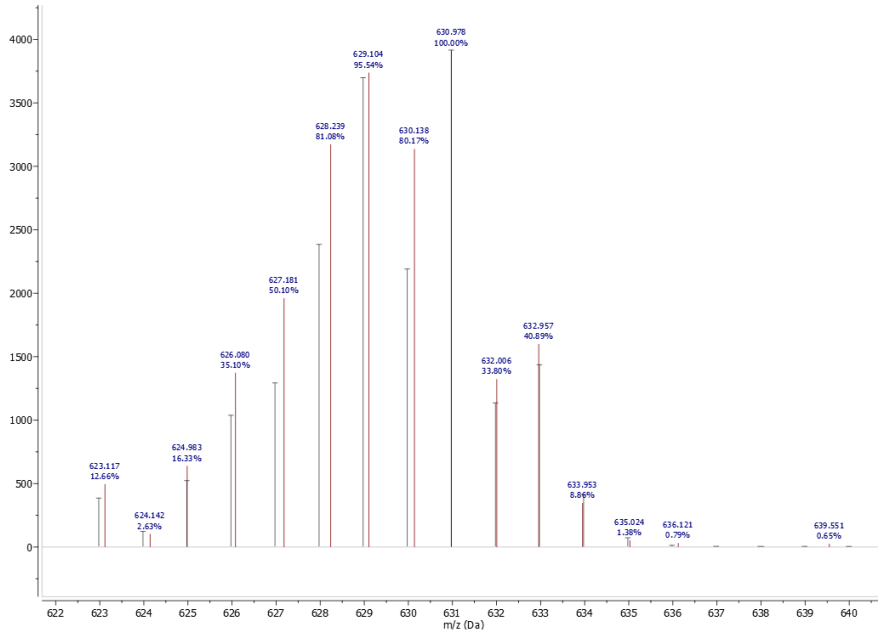

Figure S20 ESI-MS spectrum of complex [Ru(bipy)$_2$(4-Br-Sal)] (**3**) together with the assignment of the most significant peaks. Below is a comparison of the simulated and measured isotope pattern for the molecular peak.

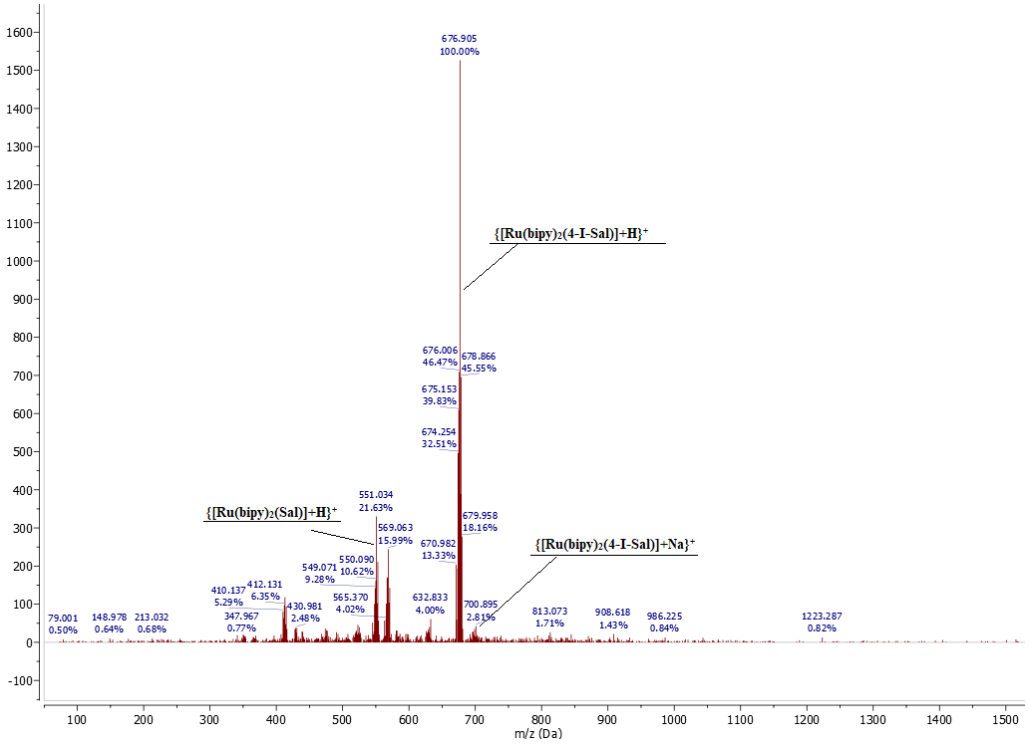

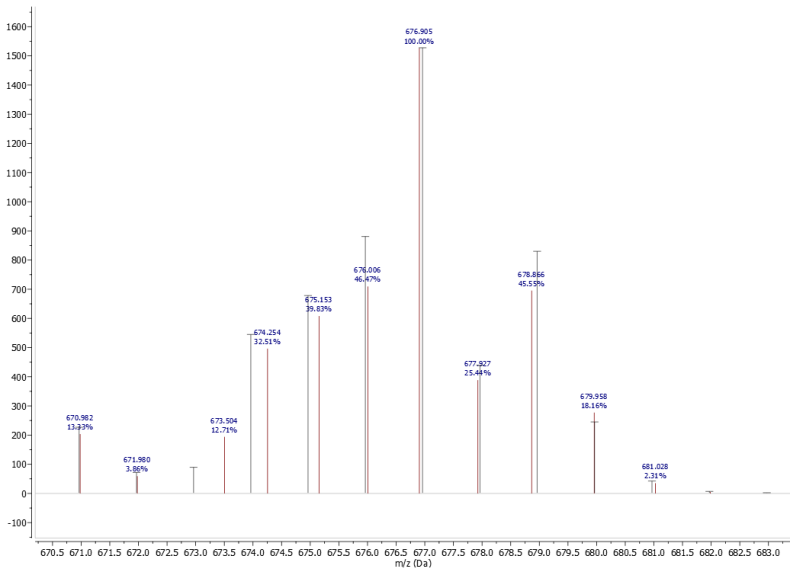

Figure S21 ESI-MS spectrum of complex [Ru(bipy)$_2$(4-I-Sal)] (**4**) together with the assignment of the most significant peaks. Below is a comparison of the simulated and measured isotope pattern for the molecular peak.

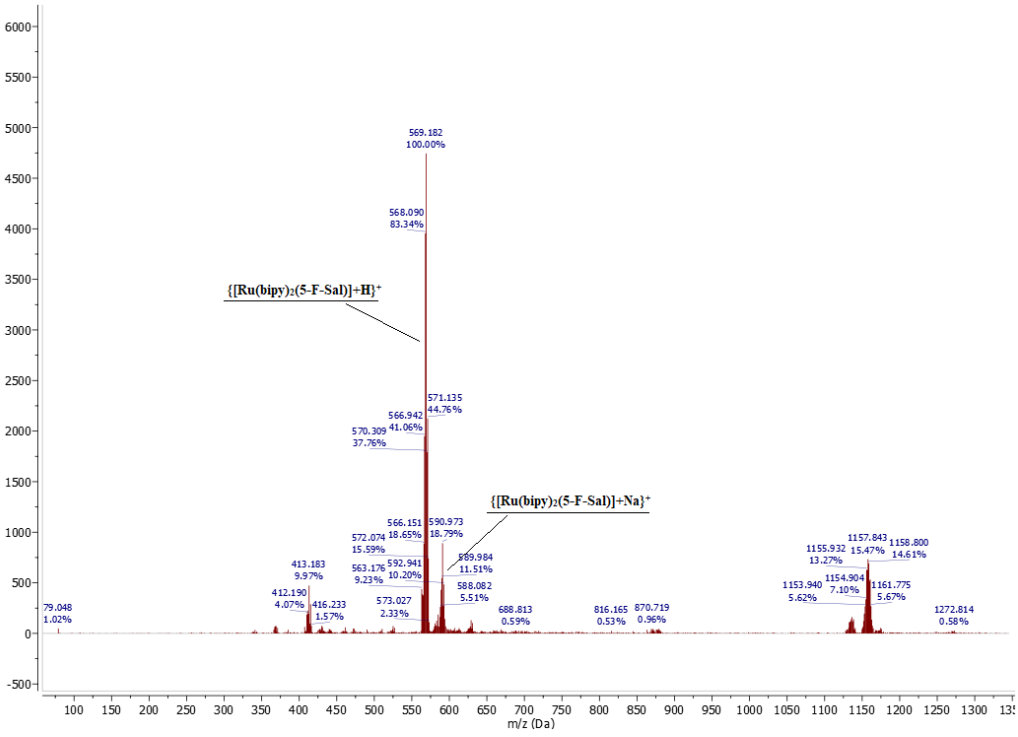

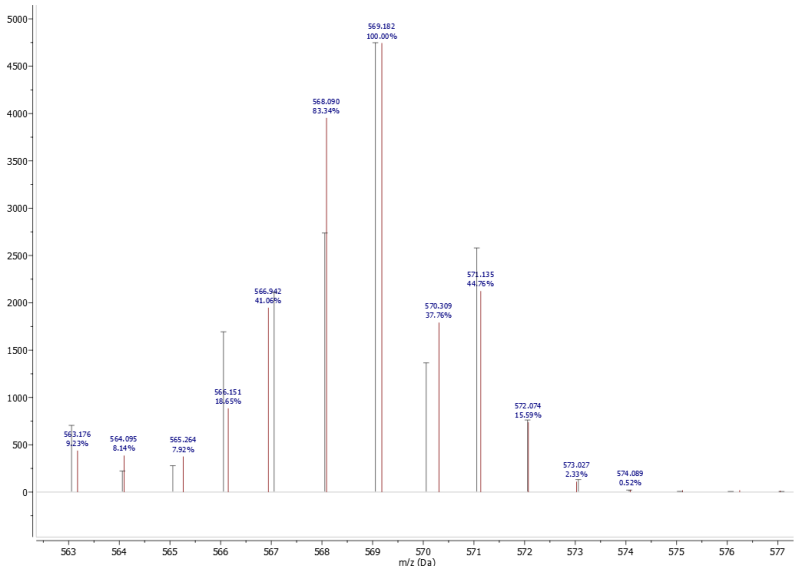

Figure S22 ESI-MS spectrum of complex [Ru(bipy)$_2$(5-F-Sal)] (**5**) together with the assignment of the most significant peaks. Below is a comparison of the simulated and measured isotope pattern for the molecular peak.

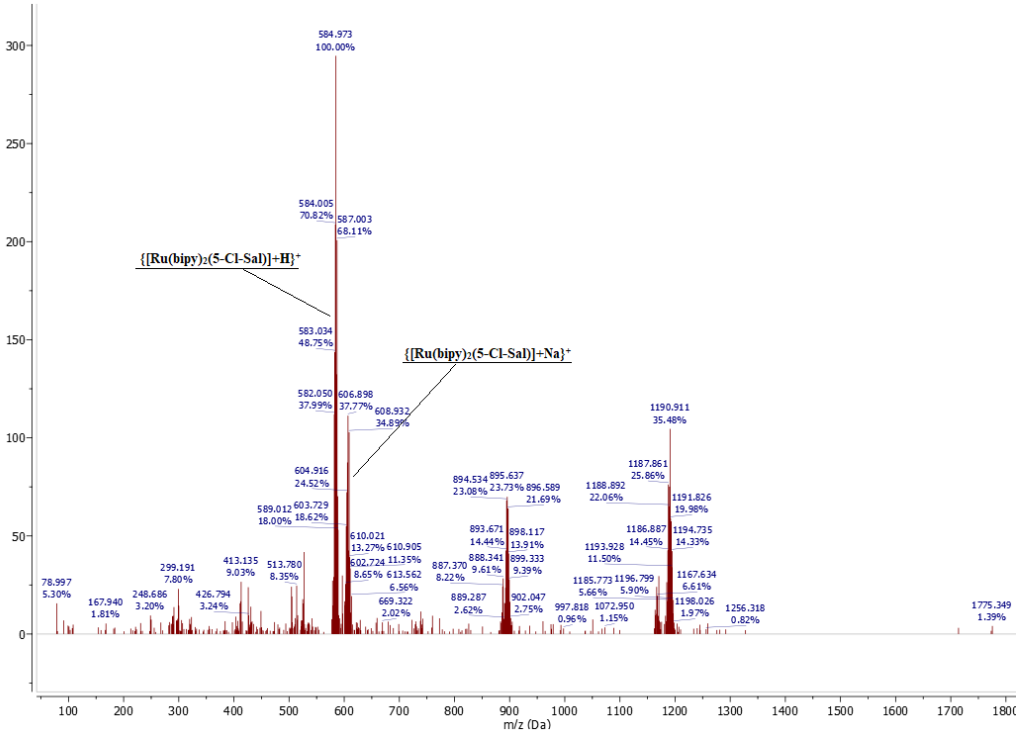

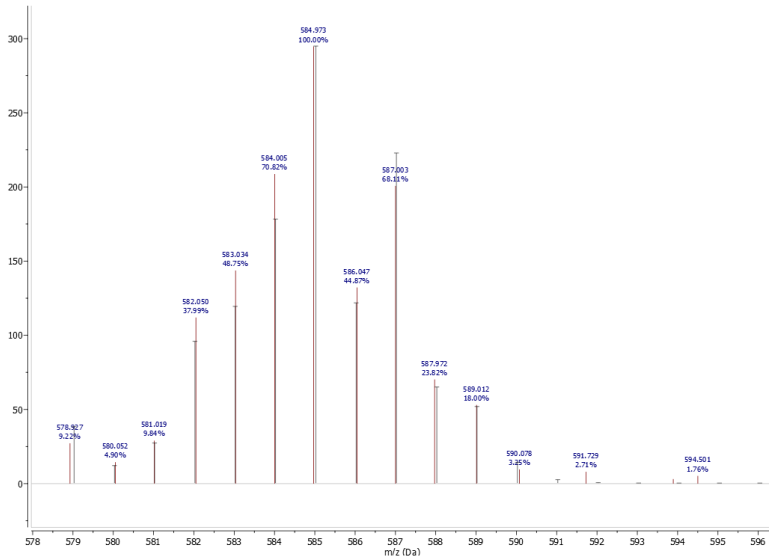

Figure S23 ESI-MS spectrum of complex [Ru(bipy)$_2$(5-Cl-Sal)] (**6**) together with the assignment of the most significant peaks. Below is a comparison of the simulated and measured isotope pattern for the molecular peak.

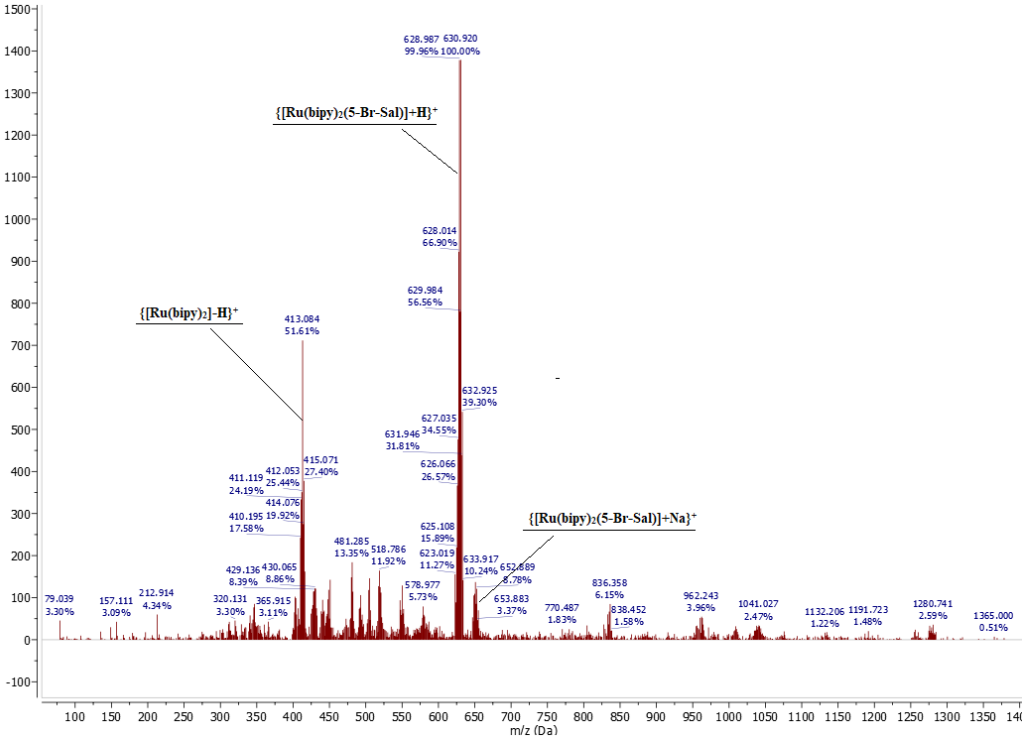

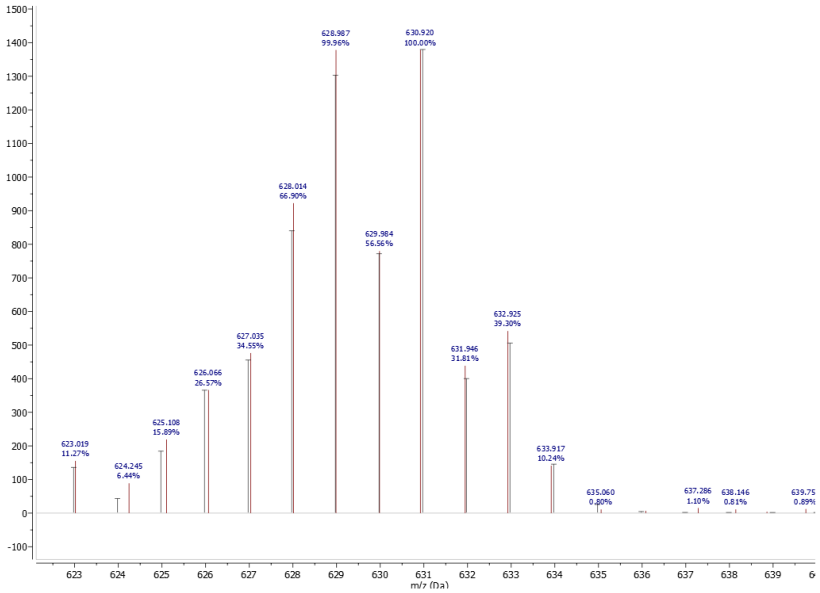

Figure S24 ESI-MS spectrum of complex [Ru(bipy)$_2$(5-Br-Sal)] (**7**) together with the assignment of the most significant peaks. Below is a comparison of the simulated and measured isotope pattern for the molecular peak.

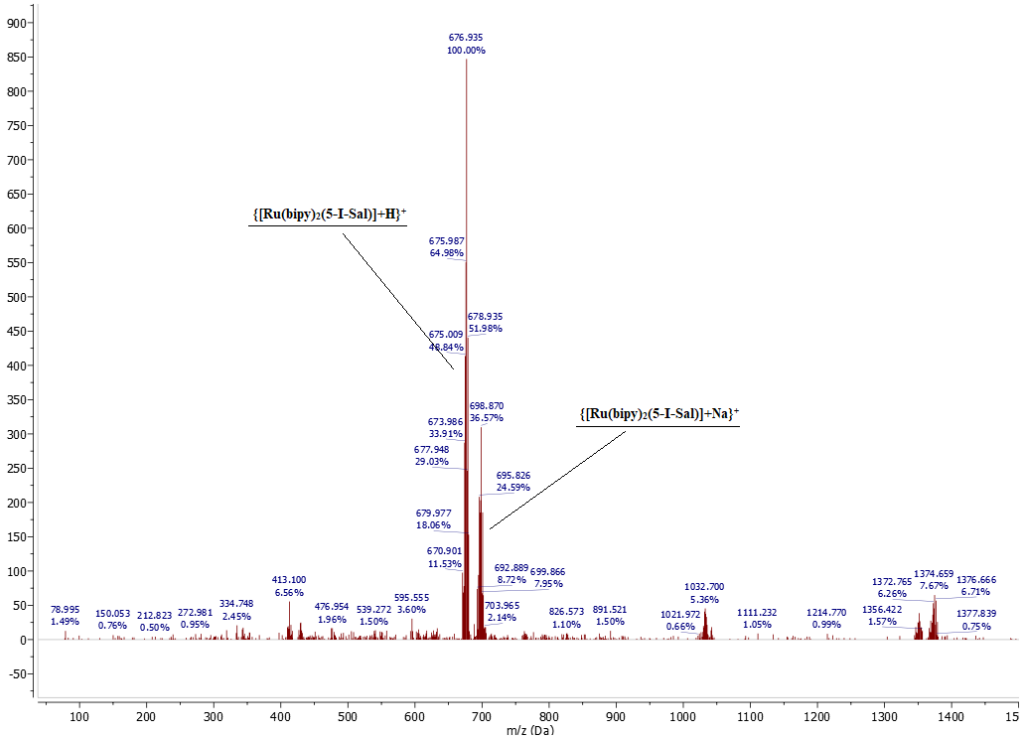

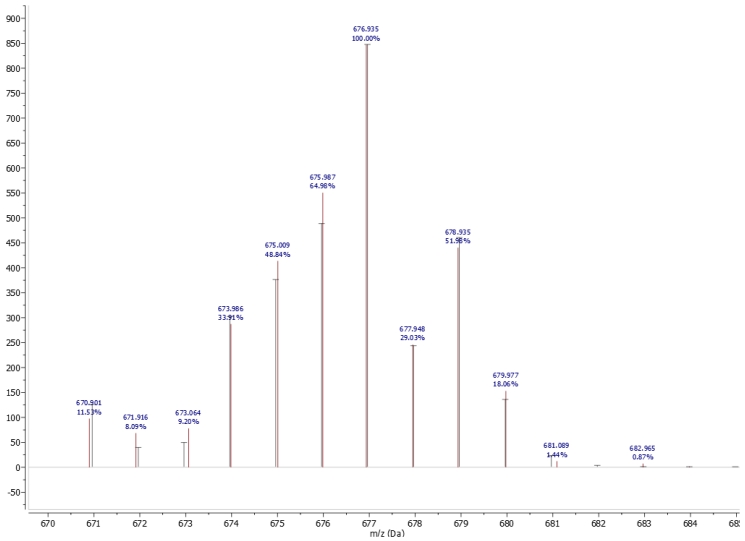

Figure S25 ESI-MS spectrum of complex [Ru(bipy)$_2$(5-I -Sal)] (**8**) together with the assignment of the most significant peaks. Below is a comparison of the simulated and measured isotope pattern for the molecular peak.

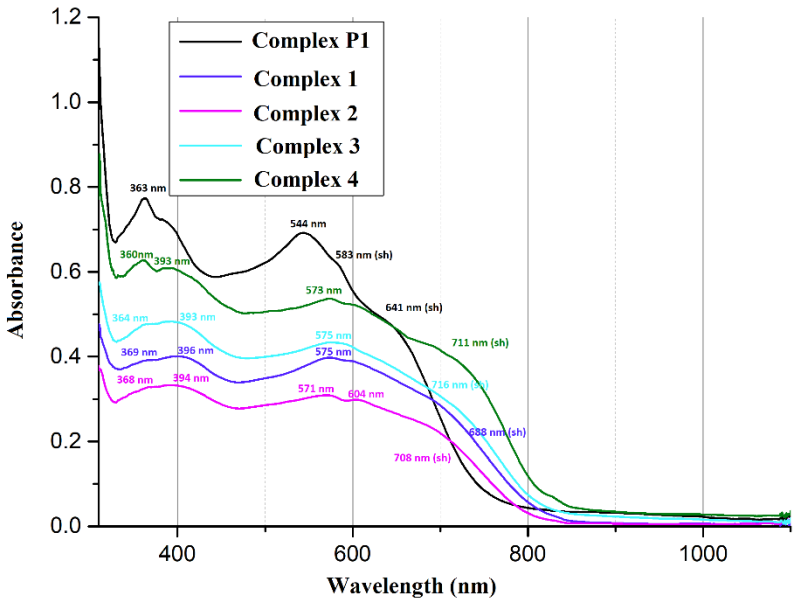

Figure S26 UV-Vis spectra of complexes **1 – 4** measured in solid state as nujol suspension.

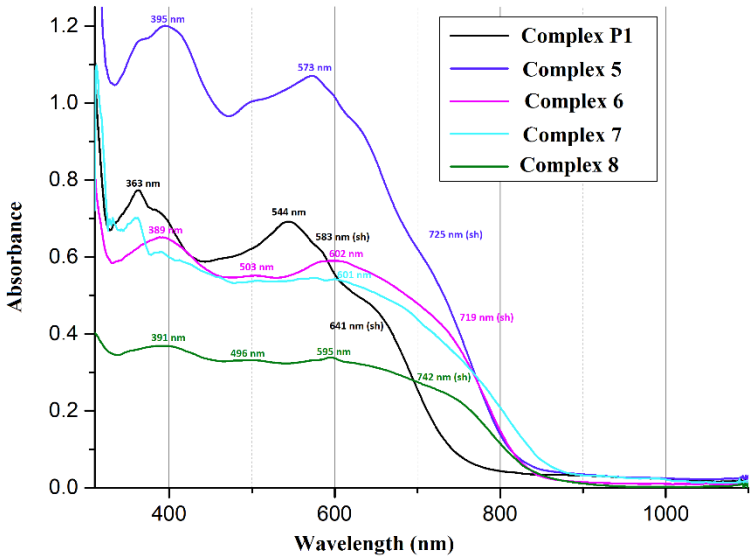

Figure S27 UV-Vis spectra of complexes **5** – **8** measured in solid state as nujol suspension.

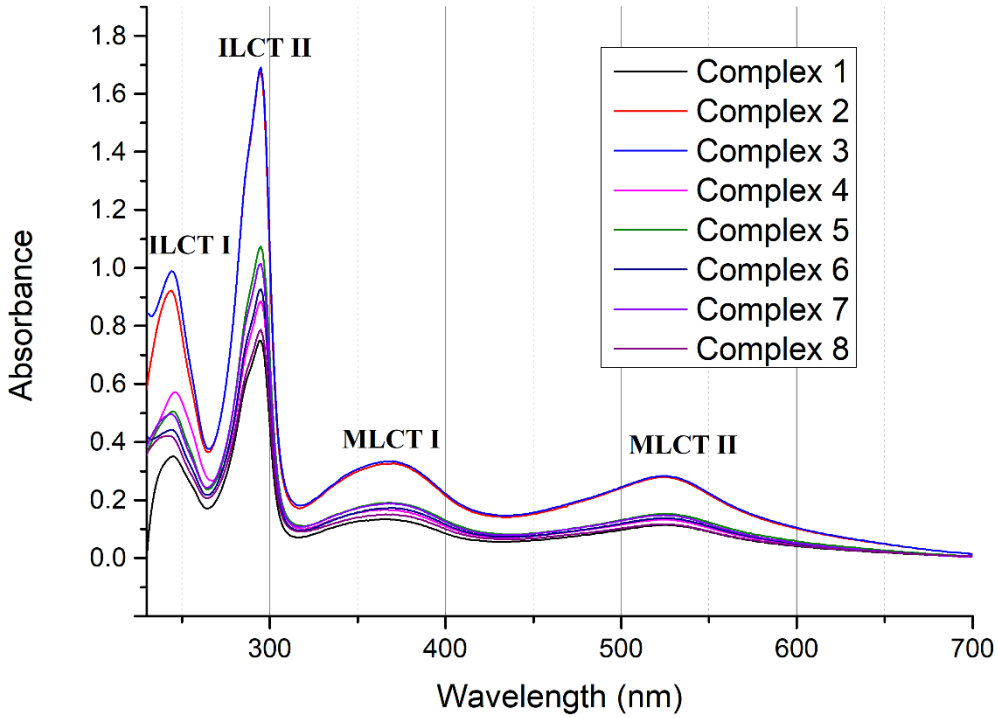

Figure S28 UV-Vis spectra of complexes **1** – **8** measured in solutions.

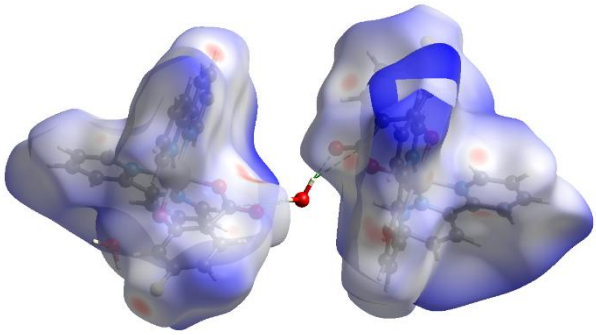

(A)

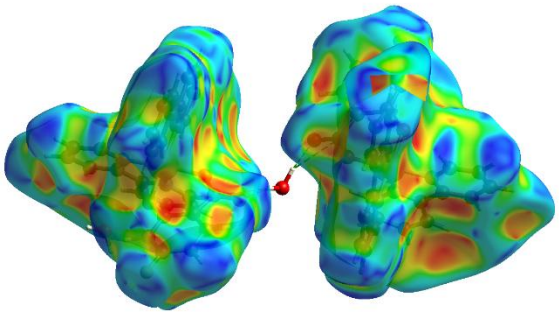

(B)

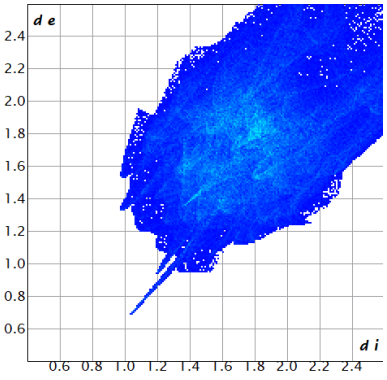
d e
d i
0.6 0.8 1.0 1.2 1.4 1.6 1.8 2.0 2.2 2.4

(C)

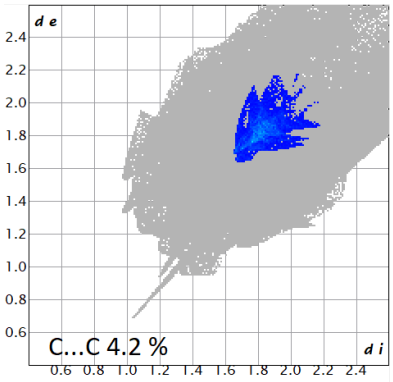
d e
C...C 4.2 %
d i
0.6 0.8 1.0 1.2 1.4 1.6 1.8 2.0 2.2 2.4

(D)

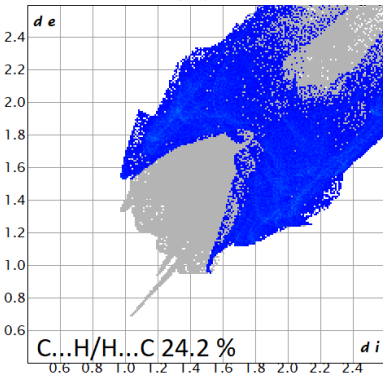
d e
C...H/H...C 24.2 %
d i
0.6 0.8 1.0 1.2 1.4 1.6 1.8 2.0 2.2 2.4

(E)

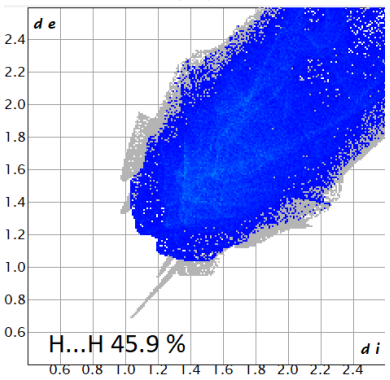
d e
H...H 45.9 %
d i
0.6 0.8 1.0 1.2 1.4 1.6 1.8 2.0 2.2 2.4

(F)

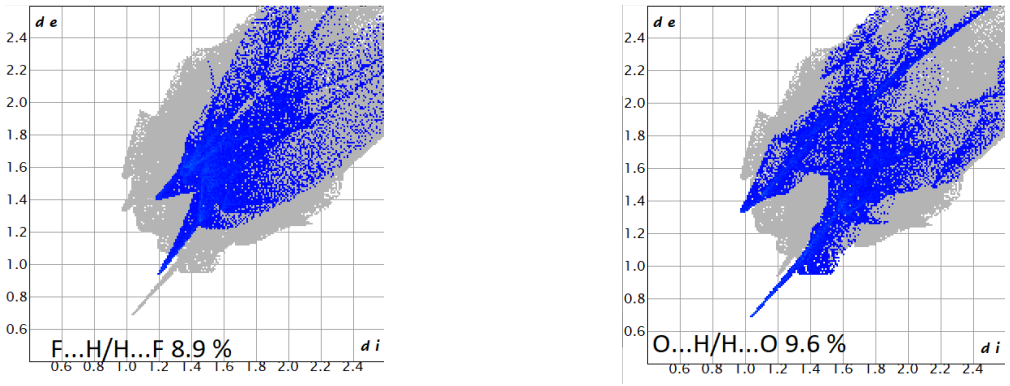

(G) (H)

Figure S29 Hirshfeld surface mapped oved d_{norm} (A) and shape index (B) for complex [Ru(bipy)$_2$(4-F-Sal)]·3H$_2$O·EtOH (**1**·3H$_2$O·EtOH) together with corresponding overall fingerprint plot (C) and plots by close contacts types: C…C (D); C…H/H…C (E); H…H (F); F…H/H…F (G) and O…H/H…O (H).

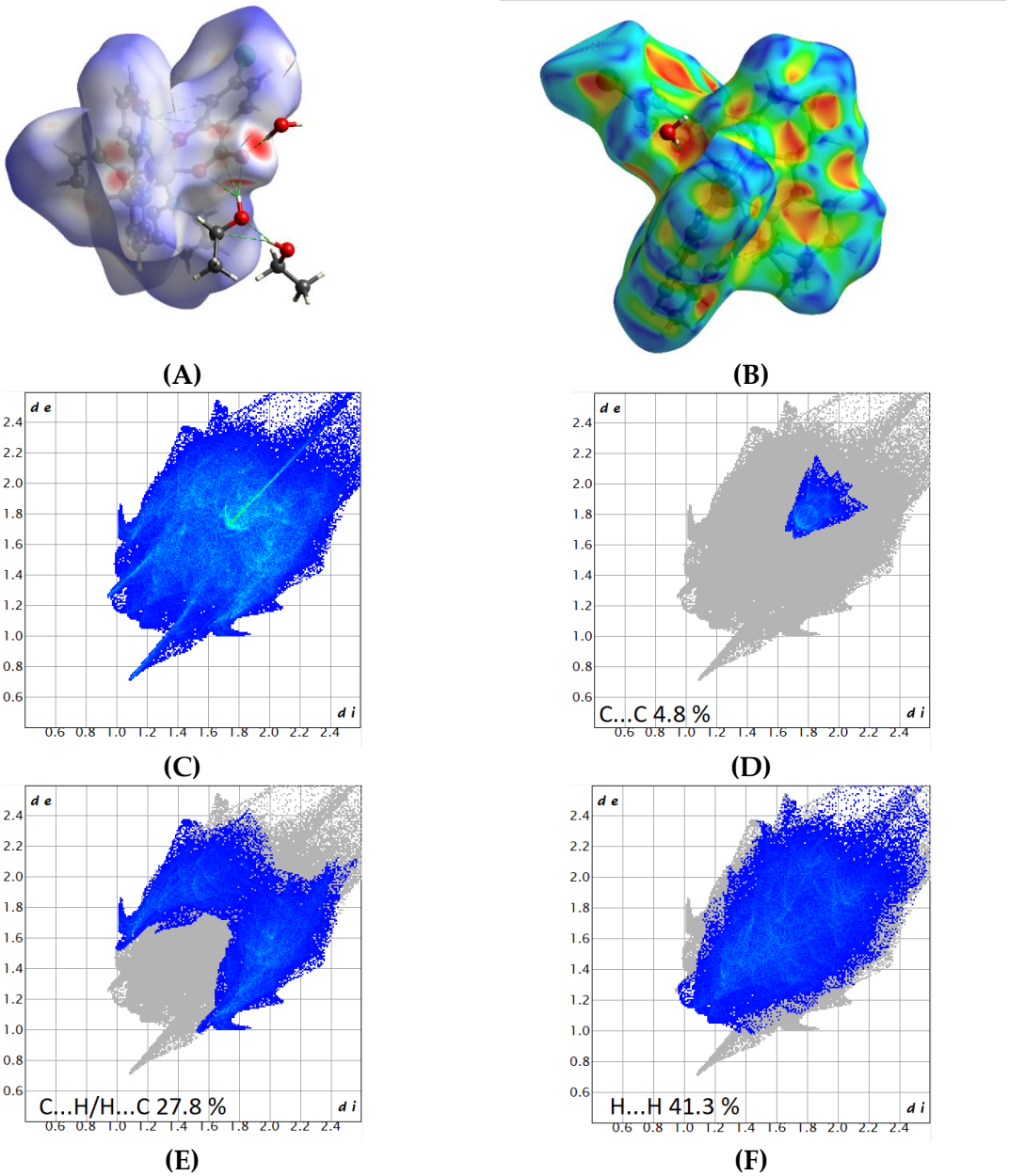

(A) (B)

(C) (D)

(E) (F)

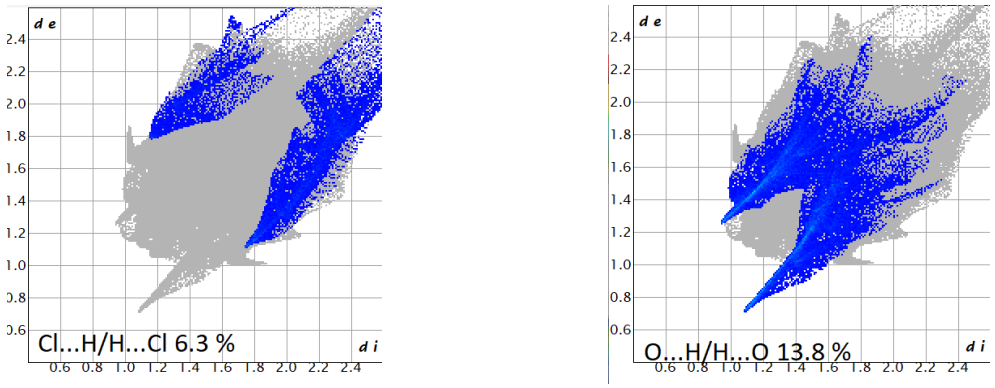

(G) (H)

Figure S30 Hirshfeld surface mapped oved d_{norm} (A) and shape index (B) for complex [Ru(bipy)$_2$(4-Cl-Sal)]·2.6H$_2$O·2EtOH (**2**·2.6H$_2$O·2EtOH) together with corresponding overall fingerprint plot (C) and plots by close contacts types: C…C (D); C…H/H…C (E); H…H (F); Cl…H/H…Cl (G) and O…H/H…O (H).

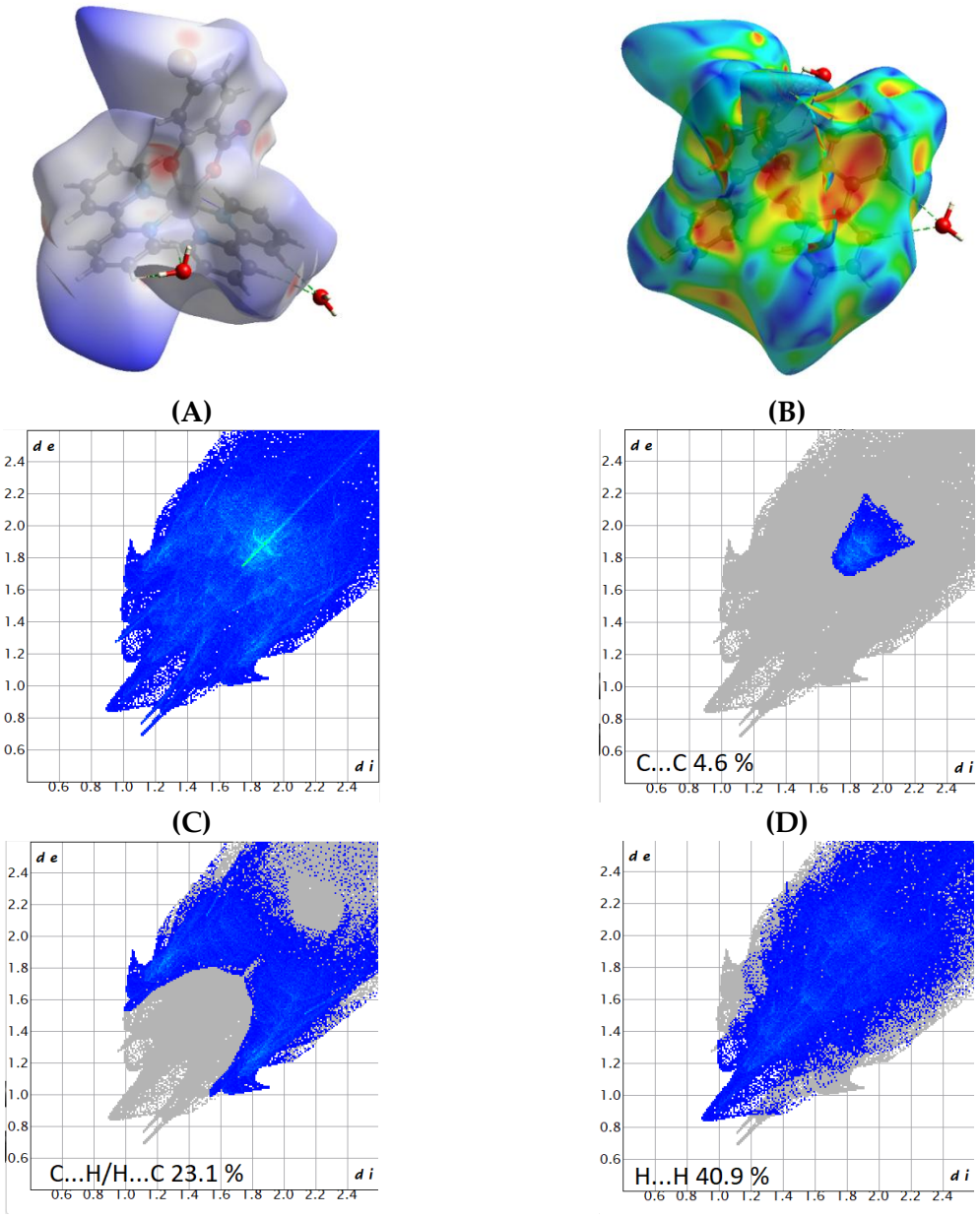

(A) (B)

(C) (D)

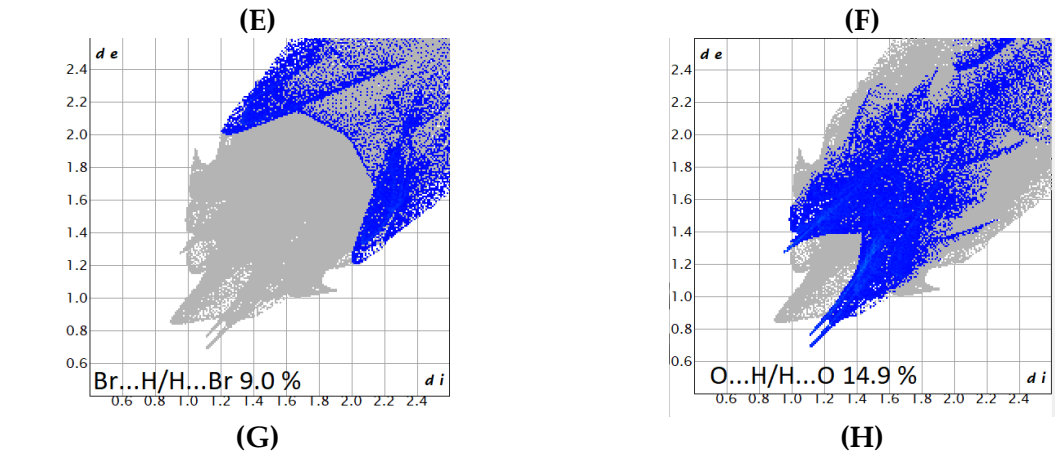

Figure S31 Hirshfeld surface mapped oved d_{norm} (A) and shape index (B) for complex [Ru(bipy)$_2$(4-Br-Sal)]·6H$_2$O (**3**·6H$_2$O) together with corresponding overall fingerprint plot (C) and plots by close contacts types: C…C (D); C…H/H…C (E); H…H (F); Br…H/H…Br (G) and O…H/H…O (H).

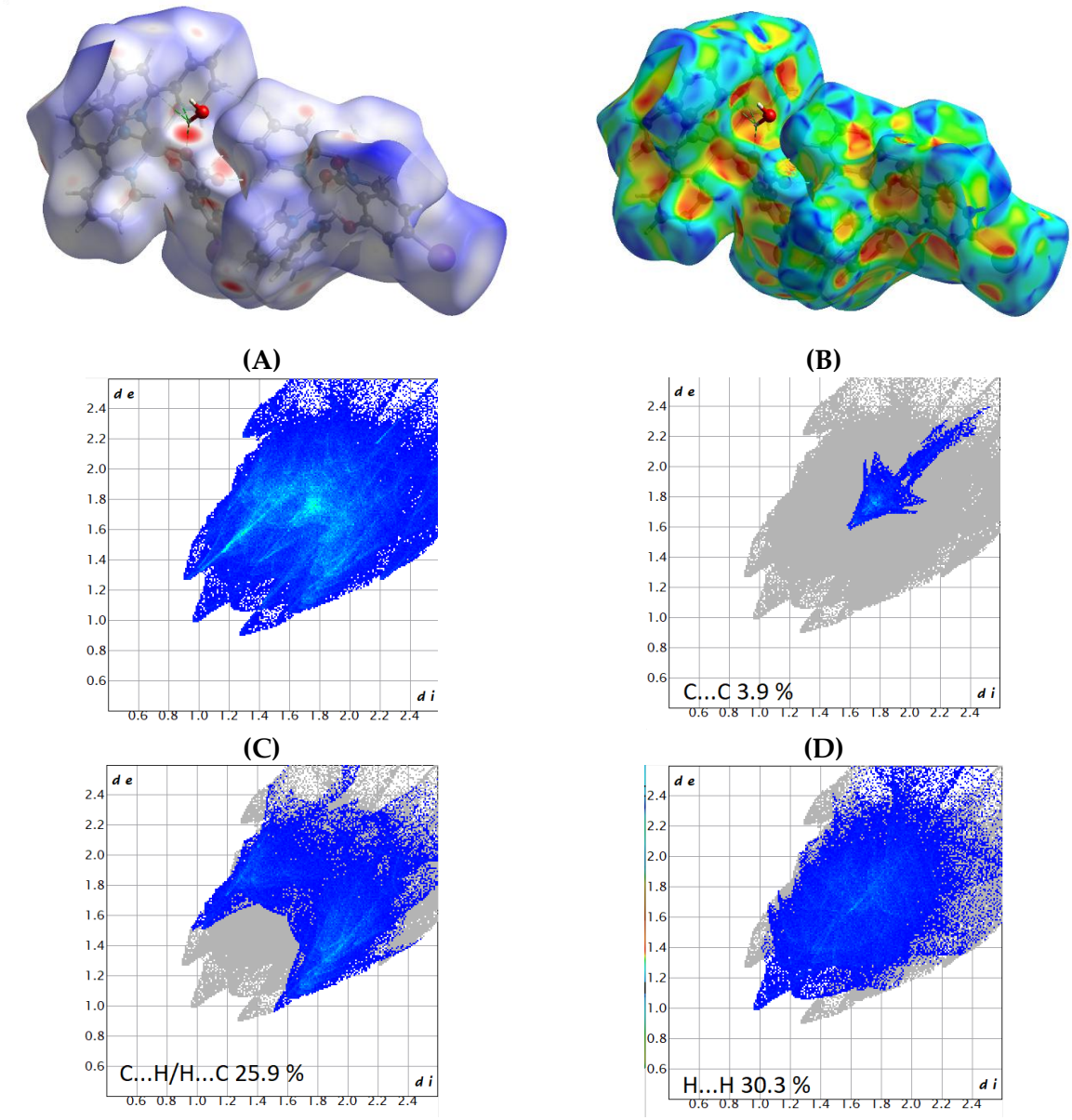

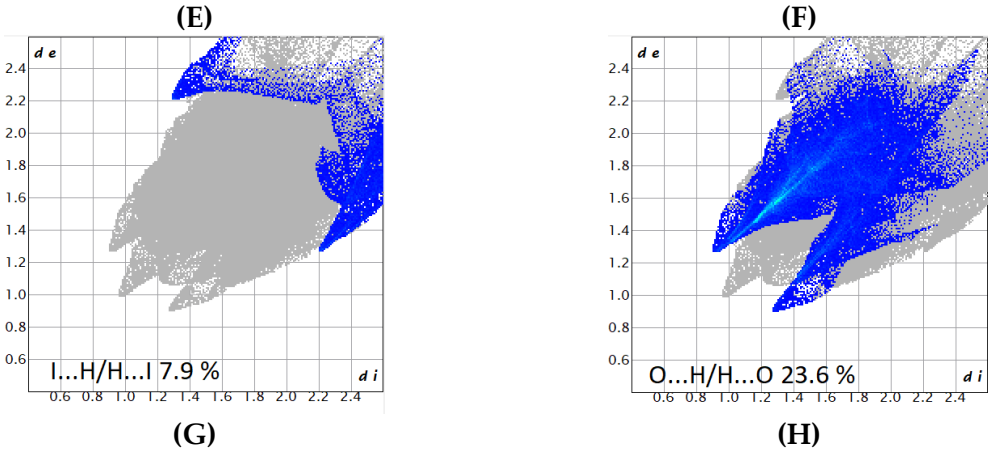

Figure S32 Hirshfeld surface mapped oved d_{norm} (A) and shape index (B) for complex [Ru(bipy)$_2$(4-I-Sal)]·3H$_2$O (**4**·3H$_2$O) together with corresponding overall fingerprint plot (C) and plots by close contacts types: C…C (D); C…H/H…C (E); H…H (F); I…H/H…I (G) and O…H/H…O (H).

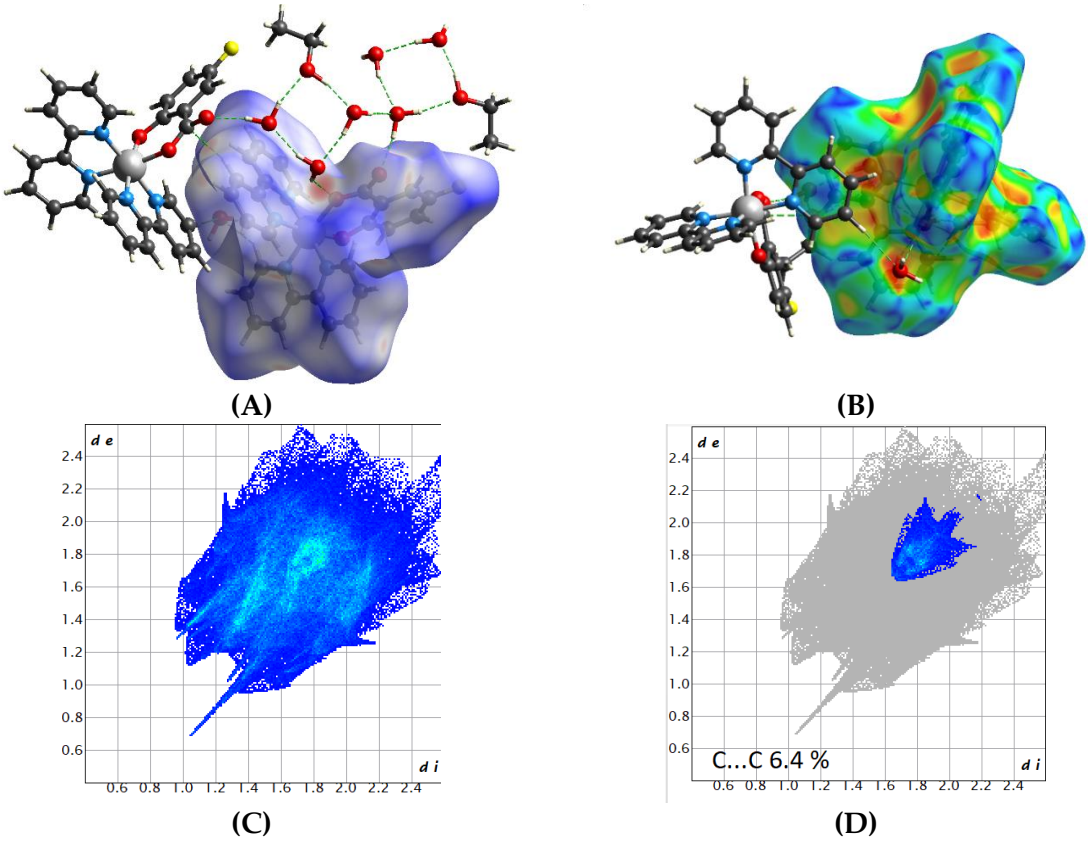

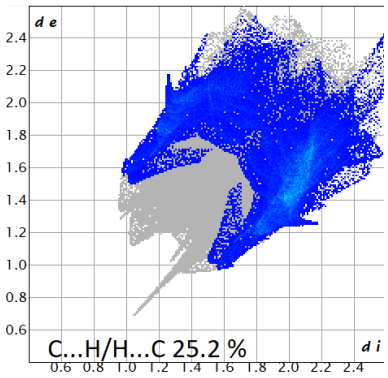

(E)

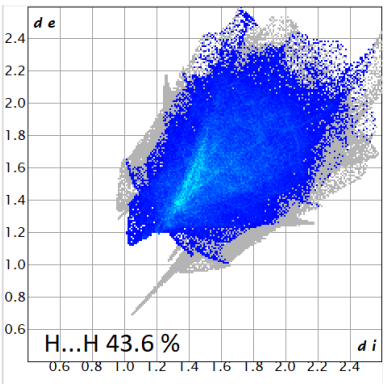

(F)

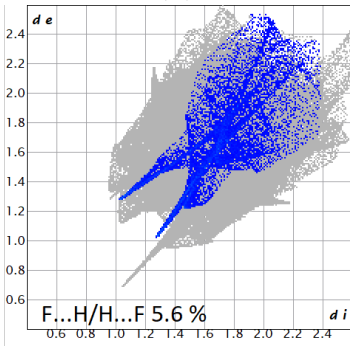

(G)

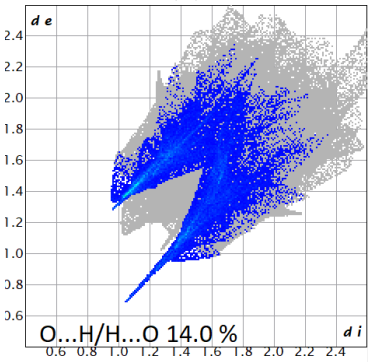

(H)

Figure S33 Hirshfeld surface mapped oved d_{norm} (A) and shape index (B) for complex [Ru(bipy)$_2$(5-F-Sal)]·1.55H$_2$O (**5**·1.55H$_2$O) together with corresponding overall fingerprint plot (C) and plots by close contacts types: C…C (D); C…H/H…C (E); H…H (F); F…H/H…F (G) and O…H/H…O (H).

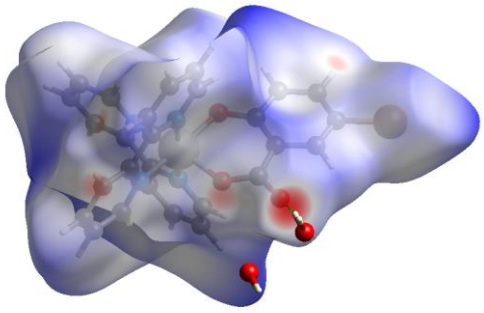

(A)

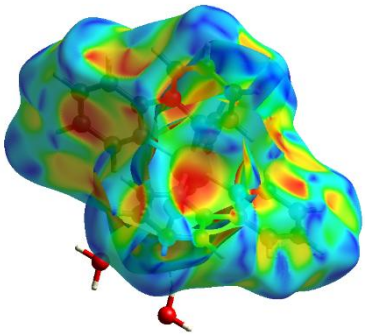

(B)

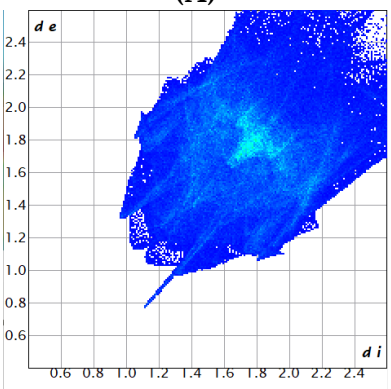

(C)

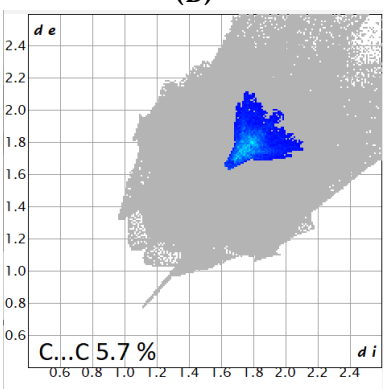

(D)

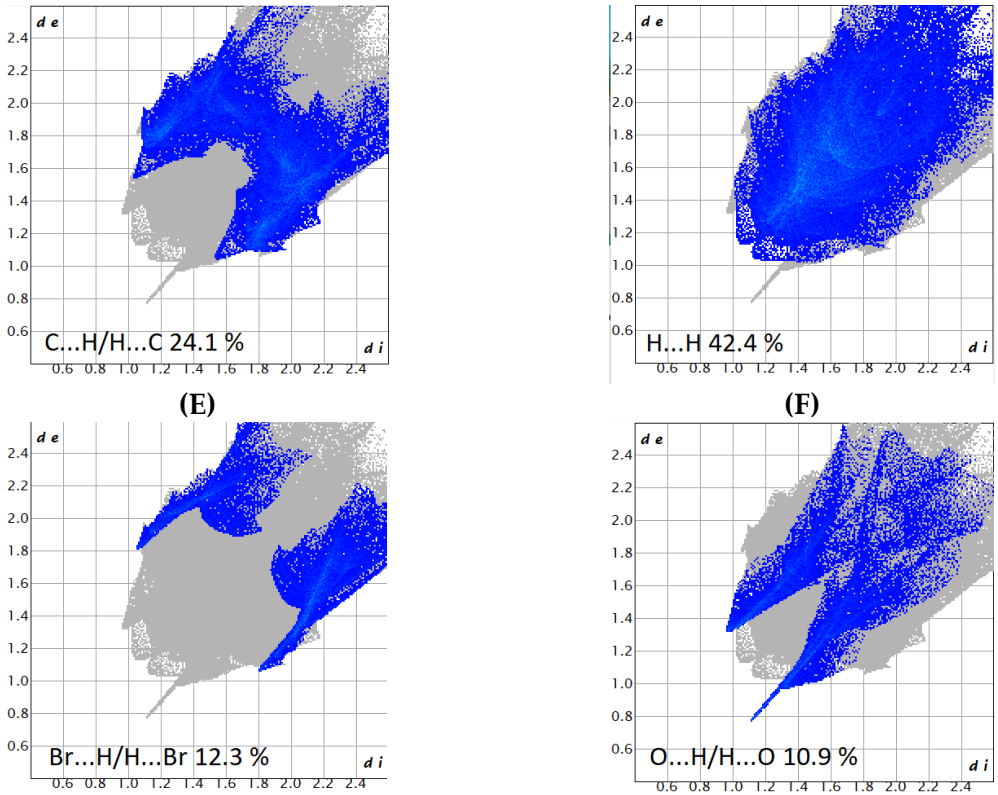

Figure S34 Hirshfeld surface mapped oved d_{norm} (A) and shape index (B) for complex $[Ru(bipy)_2(5\text{-Br-Sal})]\cdot 1.75H_2O$ (**7**·1.75H_2O) together with corresponding overall fingerprint plot (C) and plots by close contacts types: C…C (D); C…H/H…C (E); H…H (F); Br…H/H…Br (G) and O…H/H…O (H).

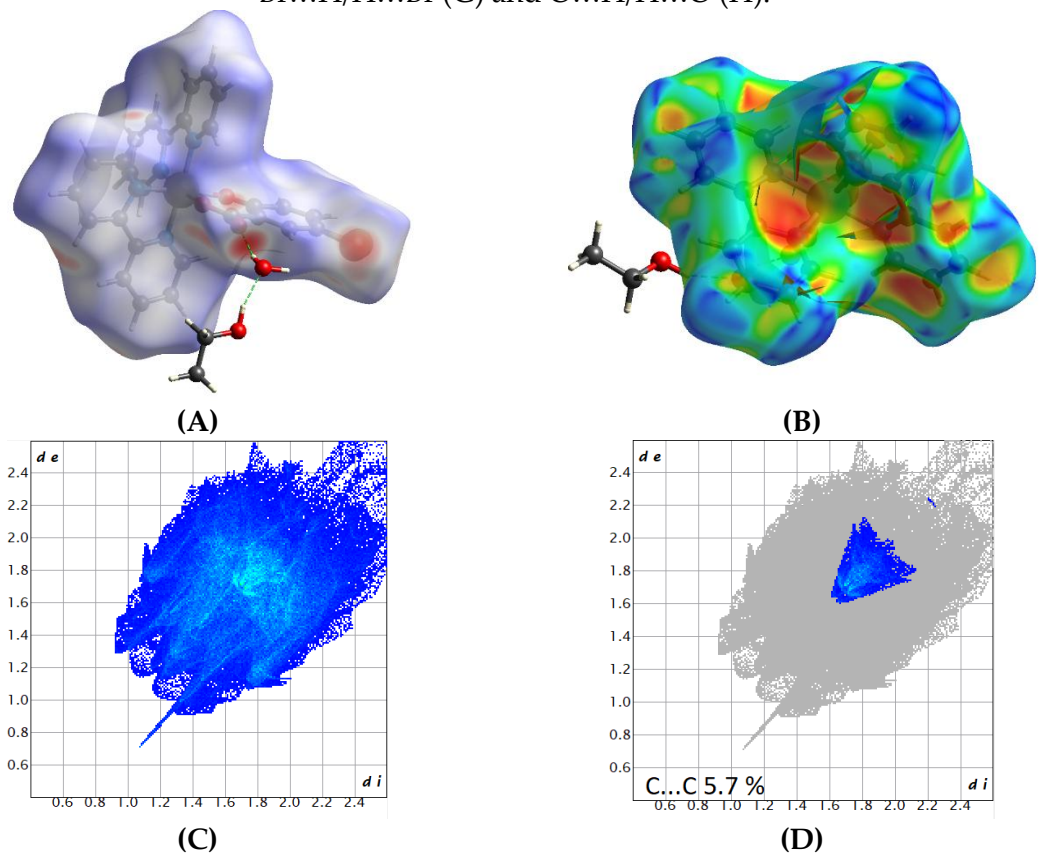

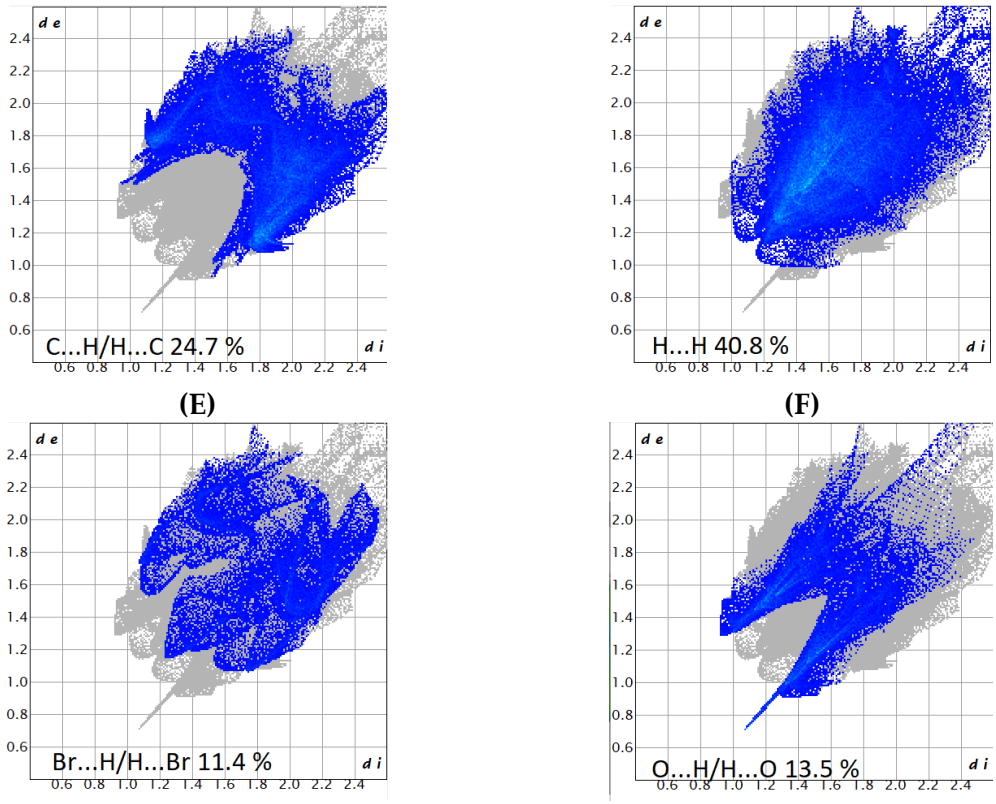

Figure S35 Hirshfeld surface mapped oved d_{norm} (A) and shape index (B) for complex [Ru(bipy)$_2$(5-Br-Sal)]·H$_2$O·EtOH (**7**·H$_2$O·EtOH) together with corresponding overall fingerprint plot (C) and plots by close contacts types: C…C (D); C…H/H…C (E); H…H (F); Br…H/H…Br (G) and O…H/H…O (H).

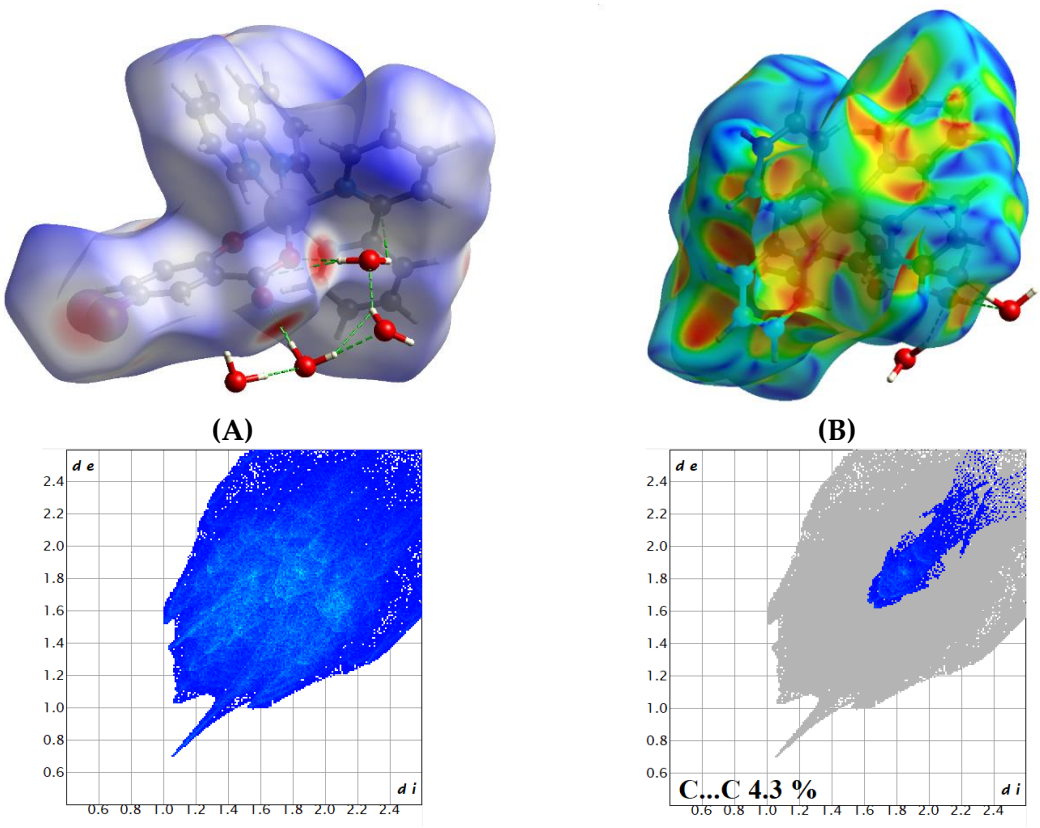

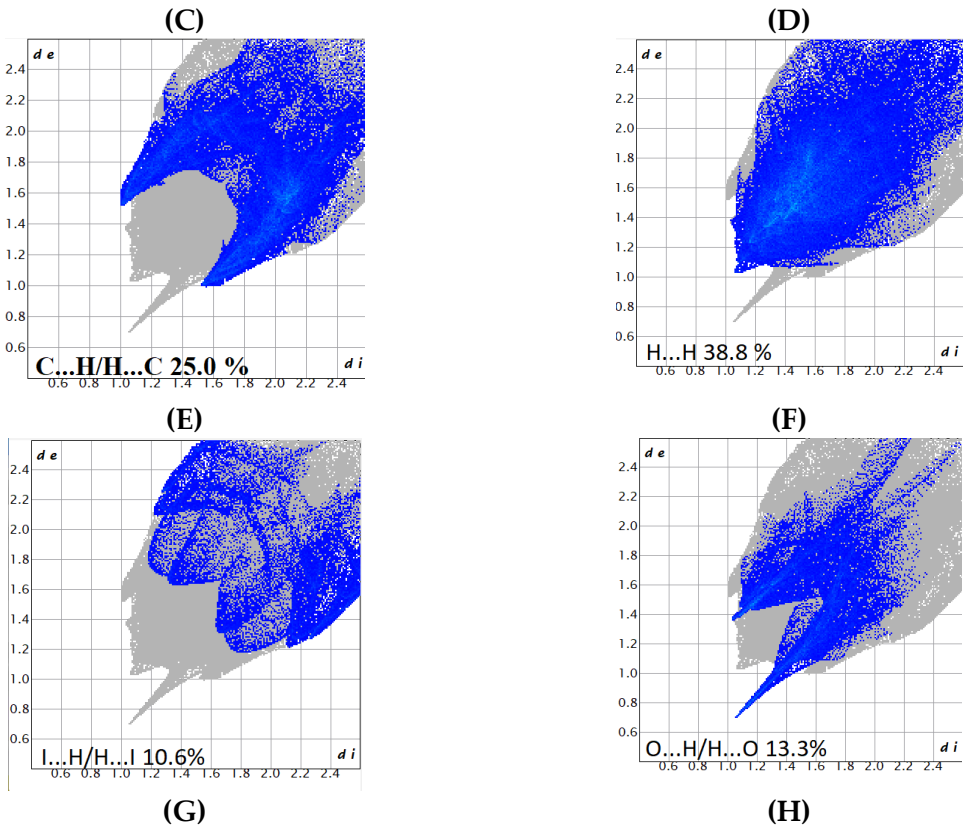

Figure S36 Hirshfeld surface mapped oved d_{norm} (A) and shape index (B) for complex [Ru(bipy)$_2$(5-I -Sal)]·4H$_2$O (**8**·4H$_2$O) together with corresponding overall fingerprint plot (C) and plots by close contacts types: C…C (D); C…H/H…C (E); H…H (F); I…H/H…I (G) and O…H/H…O (H).

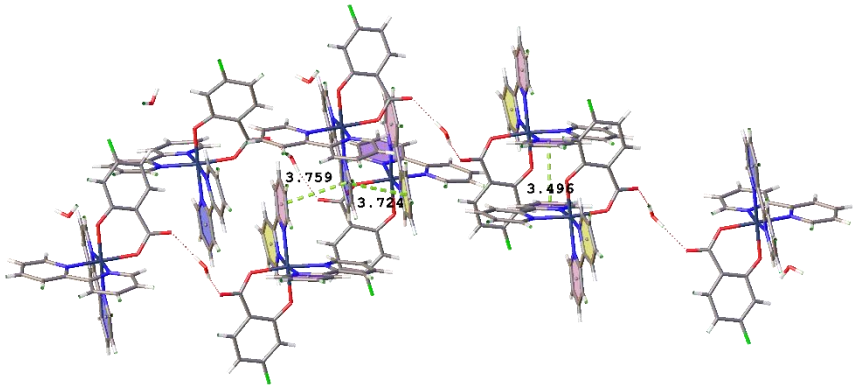

(A)

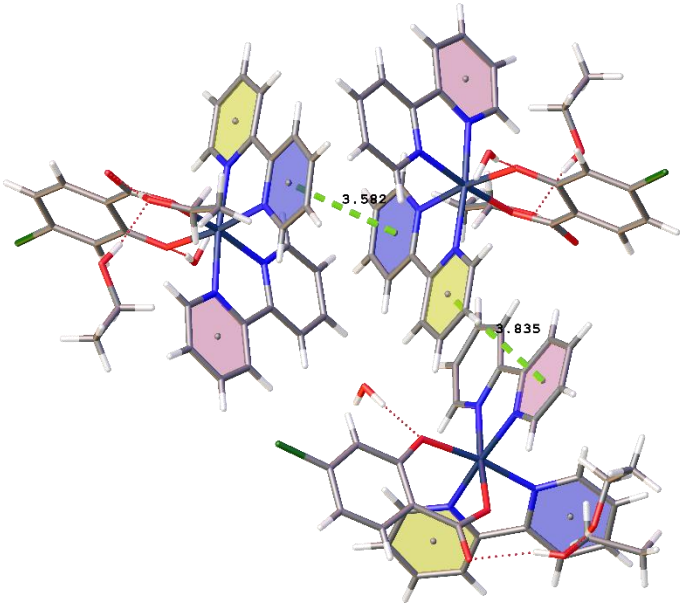

(B)

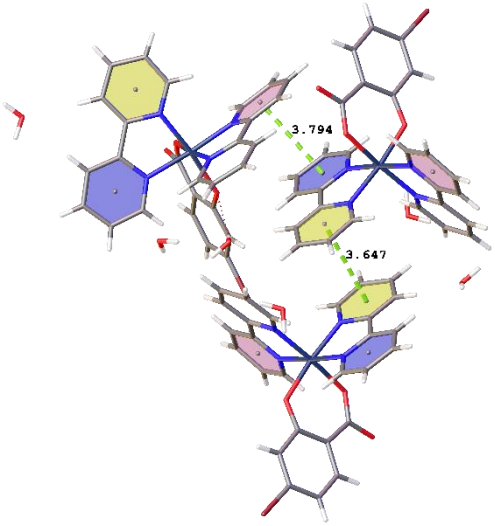

(C)

Figure S37 π···π stacking interactions for complex **1**·3H_2O·EtOH (A), **2**·2.6H_2O·2EtOH (B) and **3**·6H_2O (C).

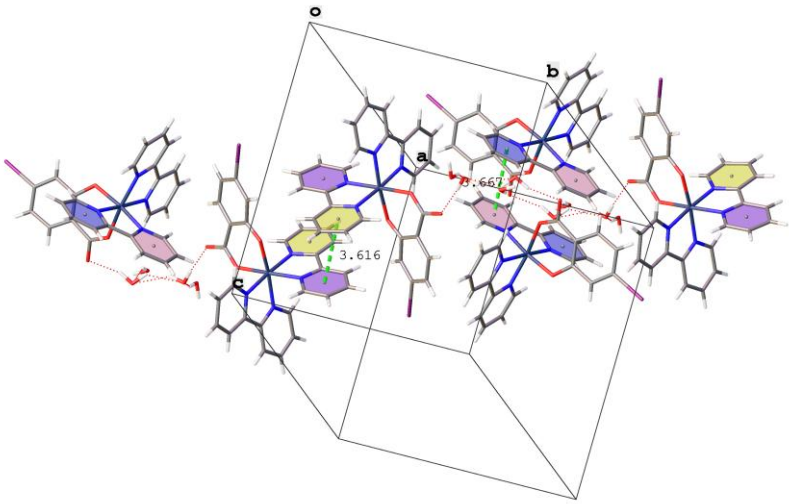

(A)

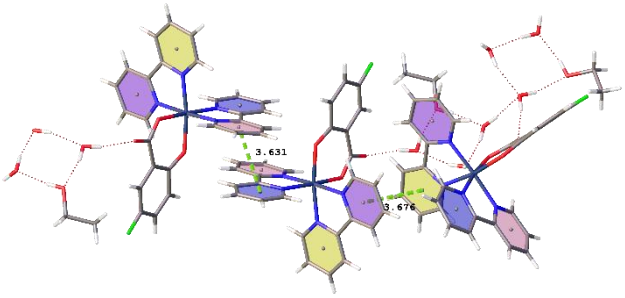

(B)

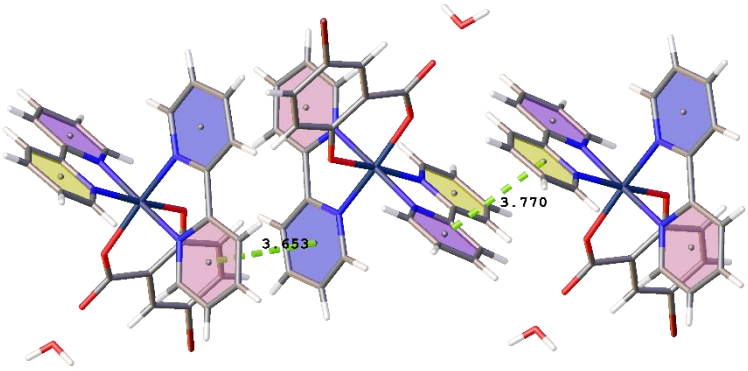

(C)

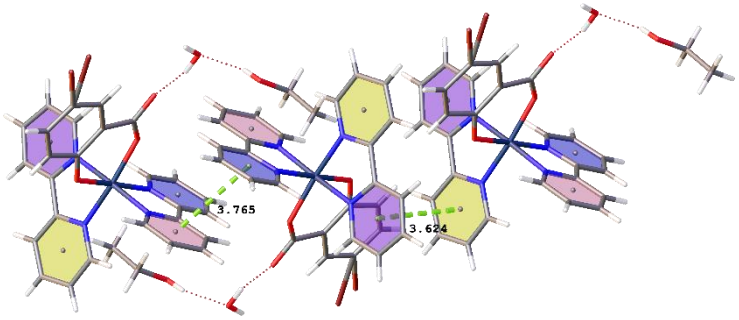

(D)

Figure S38 π···π stacking interactions for complex **4**·3H_2O (A), **5**·1.55H_2O (B), **7**·1.75H_2O (C) and **7**·4H_2O (D).

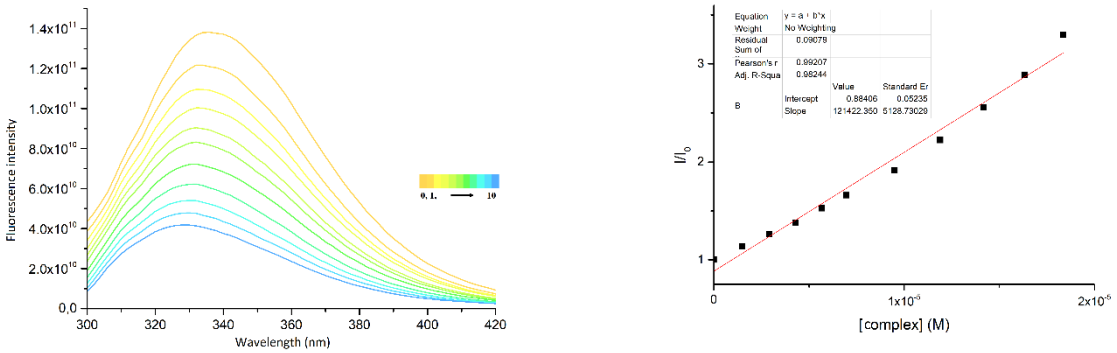

Figure S39 (A) Changes in fluorescence spectra of BSA upon complex **1** concentration rising, (B) graphical dependence of relative BSA fluorescence emission intensity (I/I_0) vs. concentration ratio [complex] .

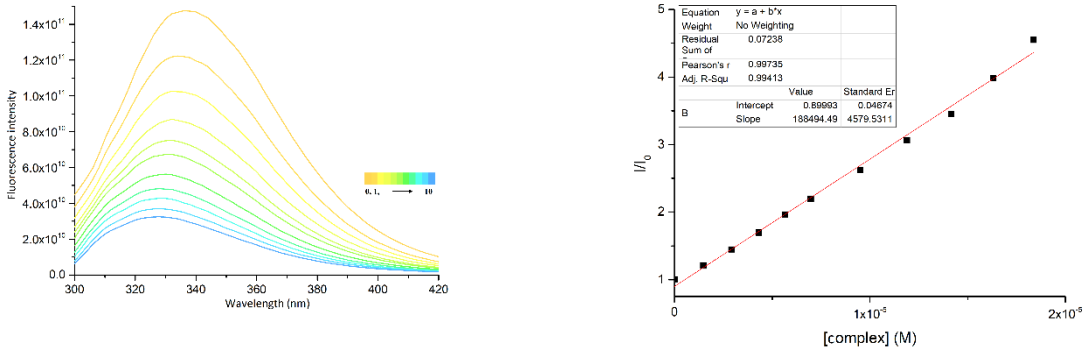

Figure S40 (A) Changes in fluorescence spectra of BSA upon complex **2** concentration rising, (B) graphical dependence of relative BSA fluorescence emission intensity (I/I_0) vs. concentration ratio [complex] .

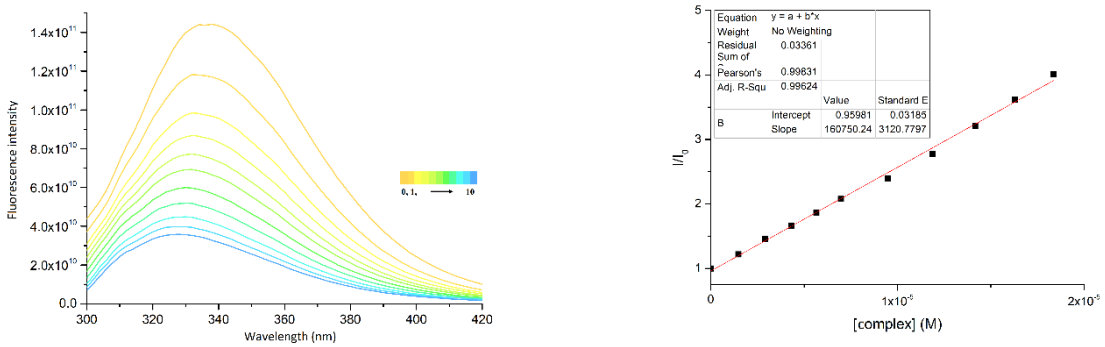

Figure S41 (A) Changes in fluorescence spectra of BSA upon complex **3** concentration rising, (B) graphical dependence of relative BSA fluorescence emission intensity (I/I_0) vs. concentration ratio [complex] .

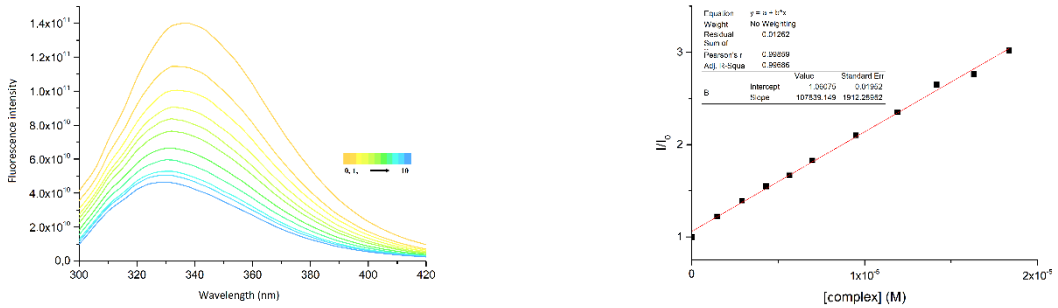

Figure S42 (A) Changes in fluorescence spectra of BSA upon complex **4** concentration rising, (B) graphical dependence of relative BSA fluorescence emission intensity (I/I_0) vs. concentration ratio [complex] .

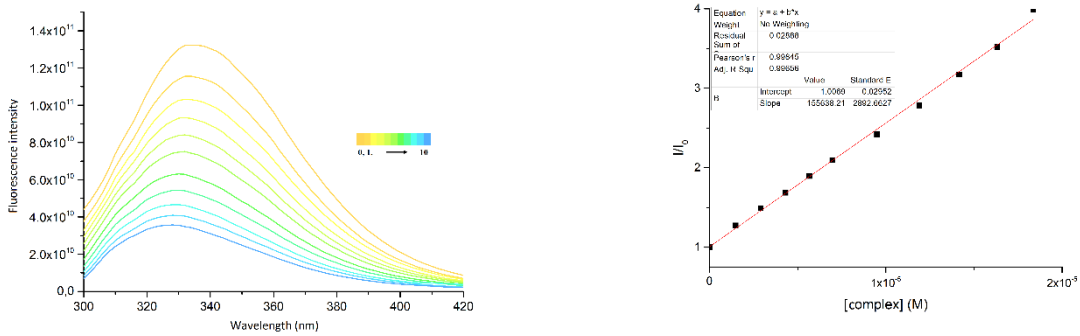

Figure S43 (A) Changes in fluorescence spectra of BSA upon complex **5** concentration rising, (B) graphical dependence of relative BSA fluorescence emission intensity (I/I_0) vs. concentration ratio [complex] .

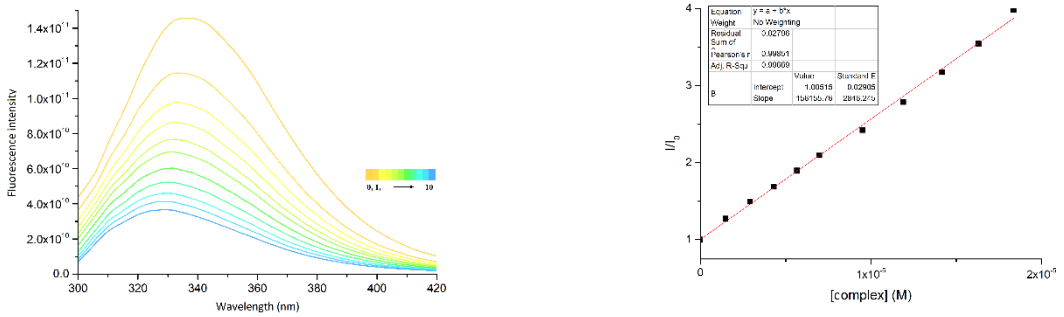

Figure S44 (A) Changes in fluorescence spectra of BSA upon complex **6** concentration rising, (B) graphical dependence of relative BSA fluorescence emission intensity (I/I_0) vs. concentration ratio [complex] .

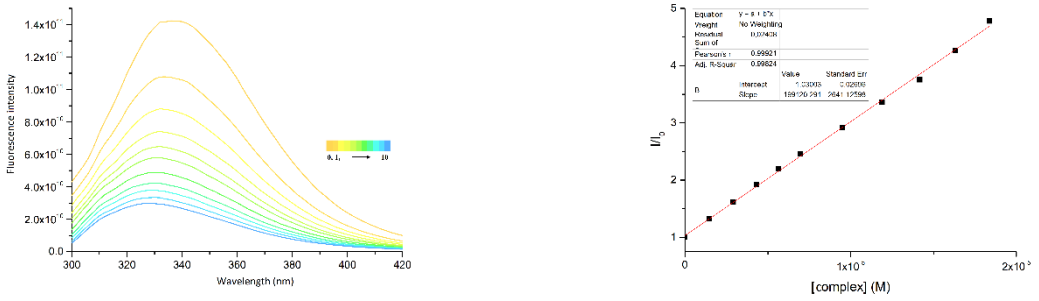

Figure S45 (A) Changes in fluorescence spectra of BSA upon complex **7** concentration rising, (B) graphical dependence of relative BSA fluorescence emission intensity (I/I_0) vs. concentration ratio [complex] .

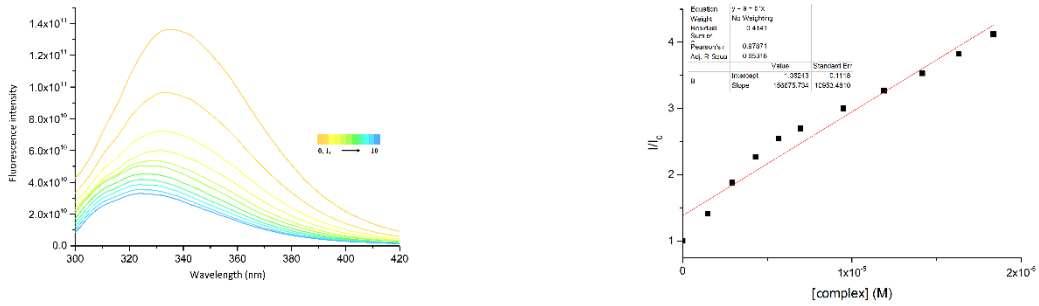

Figure S46 (A) Changes in fluorescence spectra of BSA upon complex **8** concentration rising, (B) graphical dependence of relative BSA fluorescence emission intensity (I/I_0) vs. concentration ratio [complex] .

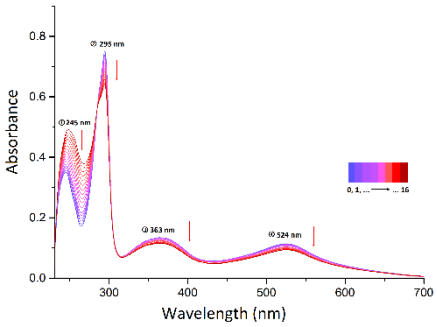
Absorbance
Wavelength (nm)
@ 295 nm
@245 nm
@ 363 nm
@ 524 nm
0, 1, ... ⟶ ... 16

(A)

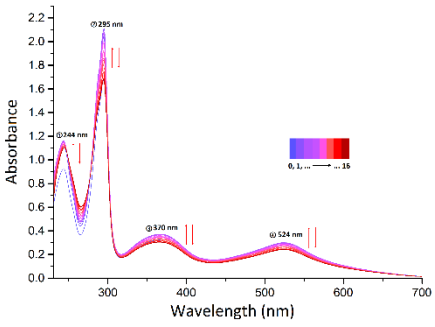
Absorbance
Wavelength (nm)
@295 nm
@244 nm
@370 nm
@ 524 nm
0, 1, ... ⟶ ... 16

(B)

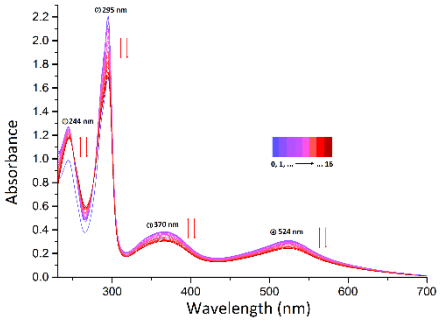
Absorbance
Wavelength (nm)
@295 nm
@244 nm
@370 nm
@ 524 nm
0, 1, ... ⟶ ... 16

(C)

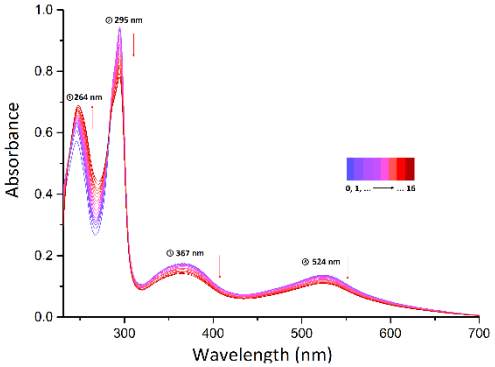
Absorbance
Wavelength (nm)
@295 nm
@264 nm
@ 367 nm
@ 524 nm
0, 1, ... ⟶ ... 16

(D)

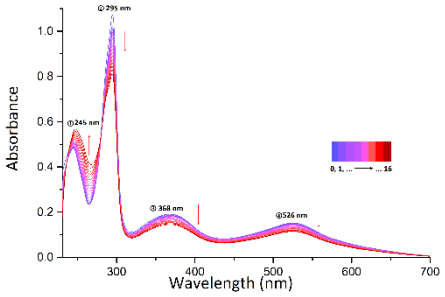
Absorbance
Wavelength (nm)
@295 nm
@245 nm
@ 368 nm
@526 nm
0, 1, ... ⟶ ... 16

(E)

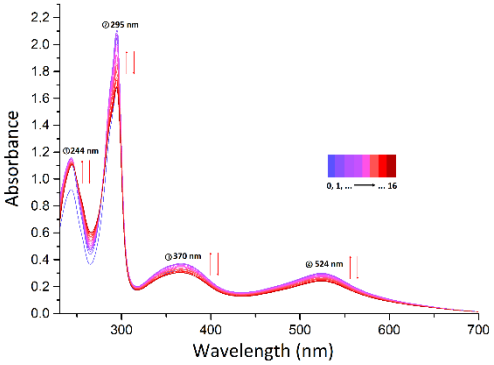
Absorbance
Wavelength (nm)
@295 nm
@244 nm
@370 nm
@ 524 nm
0, 1, ... ⟶ ... 16

(F)

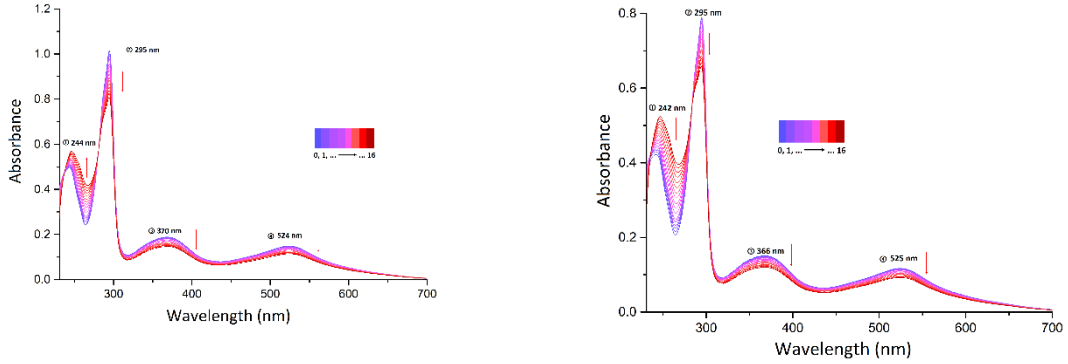

(G) **(H)**

Figure S47 Changes in the electron spectra of complexes upon addition of ct-DNA solution for complex **1** (A), **2** (B), **3** (C), **4** (D), **5** (E), **6** (F), **7** (G), **8** (H).

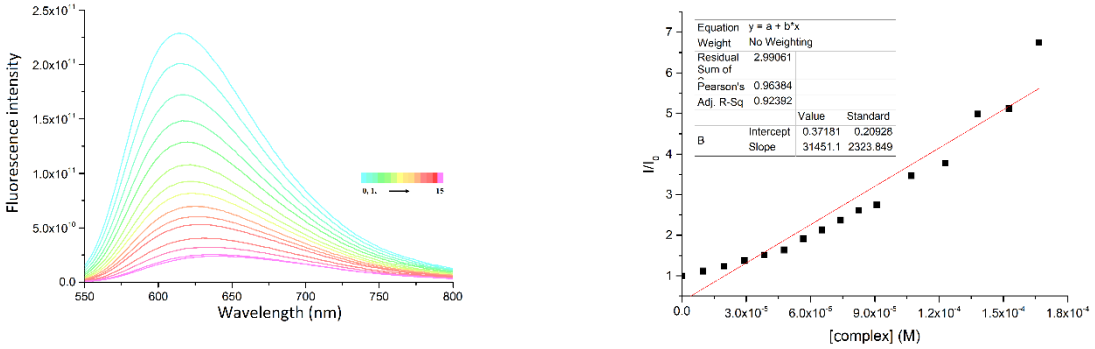

(A) **(B)**

Figure S48 (A) Changes in fluorescence spectra of EB-DNA upon complex **1** concentration rising, (B) graphical dependence of relative EB-DNA fluorescence emission intensity (I/I_0) vs. concentration ratio [complex] .

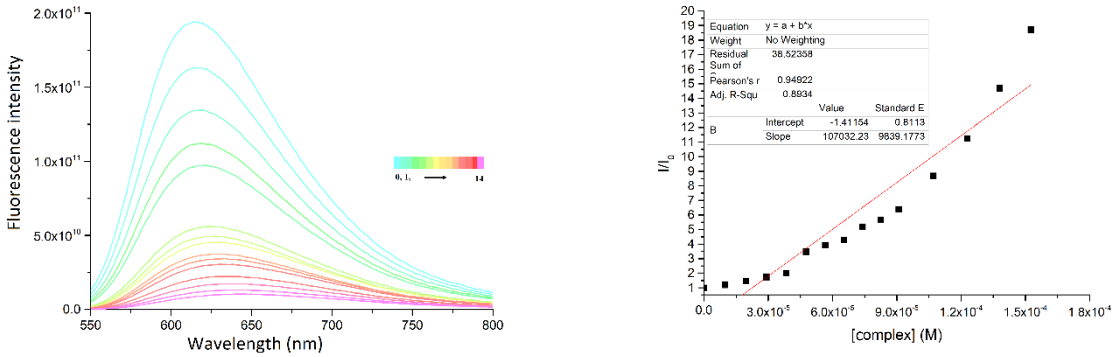

(A) **(B)**

Figure S49 (A) Changes in fluorescence spectra of EB-DNA upon complex **2** concentration rising, (B) graphical dependence of relative EB-DNA fluorescence emission intensity (I/I_0) vs. concentration ratio [complex] .

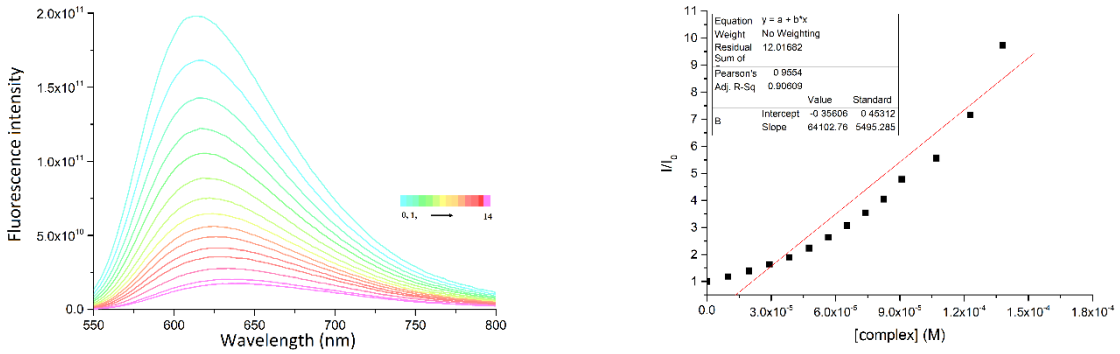

(A) **(B)**

Figure S50 (A) Changes in fluorescence spectra of EB-DNA upon complex **4** concentration rising, (B) graphical dependence of relative EB-DNA fluorescence emission intensity (I/I_0) vs. concentration ratio [complex] .

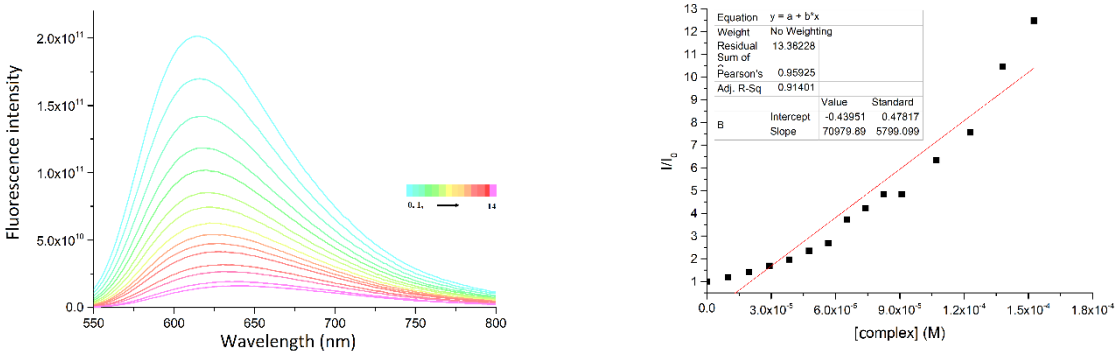

(A) **(B)**

Figure S51 (A) Changes in fluorescence spectra of EB-DNA upon complex **5** concentration rising, (B) graphical dependence of relative EB-DNA fluorescence emission intensity (I/I_0) vs. concentration ratio [complex] .

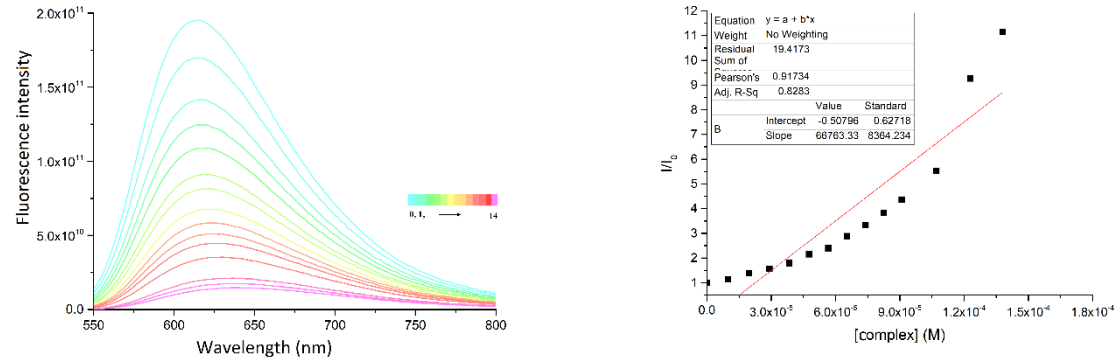

(A) **(B)**

Figure S52 (A) Changes in fluorescence spectra of EB-DNA upon complex **6** concentration rising, (B) graphical dependence of relative EB-DNA fluorescence emission intensity (I/I_0) vs. concentration ratio [complex] .

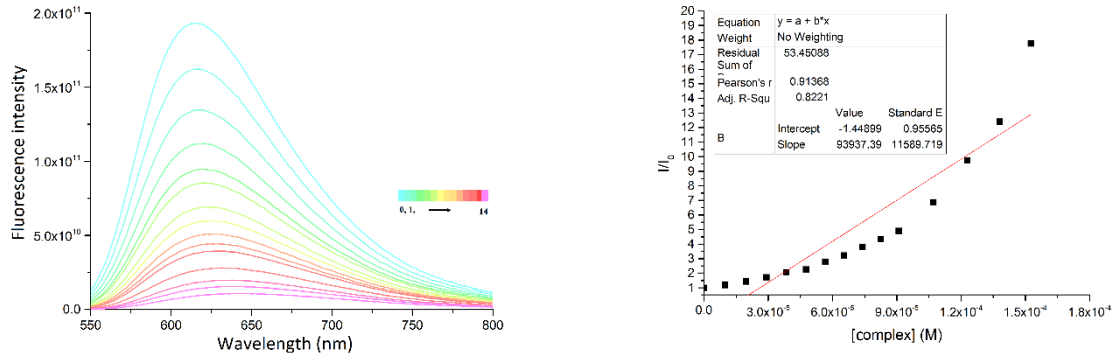

(A) **(B)**

Figure S53 (A) Changes in fluorescence spectra of EB-DNA upon complex **7** concentration rising, (B) graphical dependence of relative EB-DNA fluorescence emission intensity (I/I_0) vs. concentration ratio [complex] .

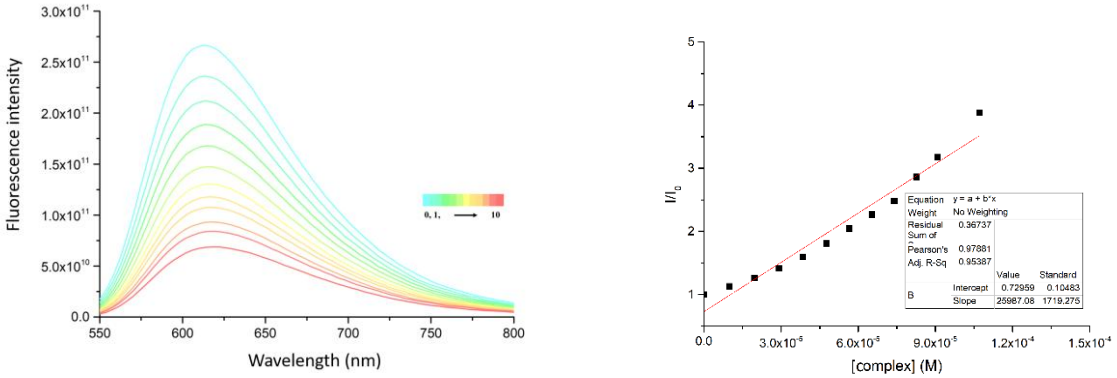

(A) **(B)**

Figure S54 (A) Changes in fluorescence spectra of EB-DNA upon complex **8** concentration rising, (B) graphical dependence of relative EB-DNA fluorescence emission intensity (I/I_0) vs. concentration ratio [complex].